DOE/PC/79863--T7

DE89 008398

MICROCRYSTALLINE IRON SULFIDE PARTICLES IN COAL: A MÖSSBAUER STUDY

by

C. C. Hinckley
G. V. Smith
Department of Chemistry and Biochemistry
and Molecular Science Program

M. Saporoschenko
Department of Physics
and Molecular Science Program

Southern Illinois University at Carbondale
Carbondale, Illinois 62901

Final Report
March 1 - December 31, 1987

Submitted to
U.S. Department of Energy
Contract Number DE-FC22-87PC79863

March 1988

DISCLAIMER

ABSTRACT

Organic sulfur can be removed from coal using a process which employs iron sulfides as in-situ catalysts. The active desulfurization catalyst is troilite, or a pyrrohotite/ troilite mixture. In this project, Mössbauer spectroscopy was used to study acid washed desulfurized chars. Mössbauer spectra of a specially prepared group of pyrrhotite standards were also analyzed. Parameter values obtained for these samples are reported and related to the iron sulfide composition. Mössbauer spectra of washed chars exhibit doublets which may be partly attributed to micro-crystalline pyrite present in the coal before treatment. Spectra of these materials have been analyzed with the help of Fourier smoothing techniques and a standard iterative method to fit Lorentzian functions to Mössbauer spectra. A sample of microcrystalline iron oxide was used as a standard to test analysis procedures. Analyses of selected low temperature char spectra confirm the presence of super-paramagnetic particles, but also indicate that they are predominantly iron oxides. Particles exhibiting internal magnetic field values characteristic of pyrrhotites are present in the samples in low concentrations. Approximately half of the spectra observed in the chars is due to nonmagnetic iron compounds.

INTRODUCTION

Iron sulfides are catalysts for coal desulfurization, and finely distributed catalyst may be an important contributing factor in the highly effective removal of organic sulfur which characterizes the Carbon Monoxide/Ethanol Desulfurization method (Webster et al. 1985). In this project, desulfurized chars derived from the above process were studied with Mössbauer spectroscopy. Most iron sulfides have been removed from the sample chars by an acid washing procedure. Still, iron Mössbauer spectra are observed for the samples. It is surmised that part of the observed Mössbauer absorptions are due to superparamagnetic particles. Spectral studies at low temperatures (4.3K) provide a means to establish the presence of superparamagnetic troilite or pyrrhotite and to estimate the particle sizes of the microcrystalline iron sulfides.

The objective of this research project is to employ Mössbauer spectroscopy to examine microcrystalline iron sulfides in coal chars to determine the extent to which highly dispersed iron sulfide catalysts may be present in the chars. These particles are the supposed remnants of iron pyrrhotites prepared during the desulfurization process. They are derived from pyrite present in the coal. This objective included the preparation and analysis of appropriate standards.

This final report summarizes the results of experiments performed on all sample types. Collection of data for iron sulfide standards, for one microcrystalline iron oxide and several chars has been completed. Analyses of the data have also been completed.

METHODS

Iron sulfide preparations

In this project, several samples of iron sulfides were obtained by reducing pyrite FeS_2, to troilite FeS using hydrogen and carbon monoxide. The pyrrhotites that were obtained as intermediate products are Fe_7S_8, Fe_8S_9, and $Fe_{11}S_{12}$.

The reduction of pyrite is achieved by flowing hydrogen or carbon monoxide through a microbalance reactor having pyrite in the weighing pan at temperatures in the range of 659 to 693K (Wiltowski et al. 1987). The weight of the sample is continuously monitored, and reaction rates are derived from weight changes. Unique compositions are identified by changes, at inflection points, in the rates of the reaction, and are obtained by halting the process at appropriate times. A Cahn System 113 is used in these preparations.

In the reduction of pyrite with hydrogen, there are three inflection points that occur at Fe_7S_8, Fe_8S_9, and $Fe_{11}S_{12}$. These inflection points are identified by changes in the rate of the reaction (Wiltowski et al. 1987). The overall reaction that takes place during the reduction is:

$$FeS_2 + H_2 \rightarrow FeS + H_2S \ .$$

Troilite can be reduced further and results in a mixture of iron, troilite, and a small amount of pyrrhotite.

In the case of reduction by carbon monoxide, there is only one inflection point at $Fe_{11}S_{12}$. Troilite is the final product of this reduction. The overall reaction is:

$$FeS_2 + CO \rightarrow FeS + OCS \ .$$

The reduction of pyrite with carbon monoxide begins at a temperature of 520K, while the reduction of pyrite with hydrogen begins at 600K.

Mössbauer spectroscopy.

The spectrometer used in this project is a Ranger Scientific model MS-900 Mössbauer Spectrometer. Data is collected and stored on magnetic disks using an Apple IIe computer with the appropriate software.

Low-temperature Mössbauer spectra are obtained by placing the sample in a Janis HD-700 Helium dewar, controlled with a Lake Shore Cryotronics TC-700 temperature controller. The dewar contains two cryogenic reservoirs separated by a vacuum chamber. In all experiments, the outer reservoir is filled with liquid nitrogen, whereas the inner reservoir is filled with liquid nitrogen or helium, depending upon the temperature range to be studied.

In order to insulate the Helium container from the liquid nitrogen, the wall that separates them is kept at a pressure of 10^{-7} torr by means of an ion pump. The Mössbauer spectrometer together with the ion pump are mounted on an MKS vibration-free table.

The Mössbauer source was manufactured by Amersham International. It is ^{57}Co of high specific activity and high chemical purity which has been electrodeposited on metal foil and then uniformly diffused through the matrix by annealing. The matrix which we are using is Rhodium, which is the best for most applications. It has a thickness of 6 μm, a diameter of 8 mm, and a line width of 0.098 mm/s.

The sample absorber is mounted in a specially designed holder which can accommodate samples from 40 mg to 1,000 mg. The distance between the source and absorber is 7 cm, as recommended by the manufacturer. Since the Mössbauer spectrometer is mounted in a laboratory where there are three or more researchers, a special shielding arrangement has been constructed. It consists of a cylinder of lead

and copper that surrounds the ^{57}Co source plus a castle of lead and concrete blocks. Measurements of radiation levels made with a calibrated detector show that at 50 cm from the source, only background radiation is present. The configuration of the instrument conforms to NRC safety requirements.

To maintain calibration of the spectrometer, a check of the linearity of the velocity is periodically performed using as a standard reference α-iron foil absorber of 25 micrograms per cm^2. This was done during this reporting period.

More than fifty spectra of iron were taken at fixed velocities of 9.8 mm/s and 11.3 mm/s, respectively, using as a variable the symmetry adjust. Iron spectra exhibit six hyperfine absorptions. In this type of calibration it is expected that the number of channels between peaks 2(-1/2 → -1/2) and 4(1/2 → -1/2) and between peaks 3(-1/2 → 1/2) and 5(1/2 → 1/2) should be equal. The position of the peaks of each spectrum was found in situ, making use of a modified non-iterative method for fitting Lorentzians to Mössbauer spectra developed by Mukoyama and Vegh (1980). The standard method (MOSFIT) for fitting Lorentzians to the experimental spectra makes use of an iterative non-linear least-squares method. Starting from the initial estimates of the parameters, new estimates are found with least-squares procedures and tested for convergence. These values serve as the bases for the next iteration, in the final values when convergence criteria are met. Our method linearizes the Lorentzian function with respect to the parameters and then makes a linear-squares fitting. For the Mössbauer spectrum, the parameters are estimated by fitting a quadratic function to the reciprocal of the experimental data. There is no need to prepare any initial estimates and there is no problem of convergence.

The six-line spectrum of a natural iron foil has been accurately measured and is widely used to measure the total velocity scan of a vibrator. Using an iron foil sample as the absorber, the spectrum observed by Mössbauer spectroscopy is used to determine the line position of the six peaks. Since it is known that the iron foil

has a magnetic splitting of 330 kG, the velocity scan has to be adjusted such that the magnetic splitting is correct. When the spectrum is adjusted in this method, the maximum velocity necessary to adjust the experimental maximum velocity to the correct line positions becomes the actual maximum velocity for all other samples run on that spectrometer. This method was used in the laboratory to calibrate the Mössbauer spectrometer.

After the spectrometer has been calibrated, the iron foil sample is replaced by an unknown sample. This sample is then analyzed using the spectrometer. The counts are collected and stored as described above. Then the parameters must be determined. The parameters are used to describe the spectrum and correspond to the hyperfine parameters, intensities, and line width. By comparing these parameters to known values, the types of multiplets contained in the sample can be determined.

Analyses of Mössbauer spectra make use of a Fortran program, MOSFIT, which uses a least squares fitting routine to find the best fit between a composite of Lorentzian absorptions and the experimental spectrum. The best fit is dependent upon parameters for the intensity of absorbtion (INT), the full width at half maximum (WID), the isomer shift (ISO), the quadrupole coupling (QUAD), and the magnetic splitting (MAG) for each separate species represented in the composite. With these parameters, the program plots a Lorentzian curve for the gamma ray absorptions and compares it with the experimental spectrum.

As an aid in spectral analysis we have developed a method that makes use of Fourier smoothing techniques (Zimmerman 1981, Aubanel and Oldham 1985). The chars which are the principal subjects of this study exhibit Mössbauer spectra which contain high levels of high-frequency noise. Fourier transformation and inversion naturally identify and eliminate noise. Noise is present at high frequencies, whereas the signal proper is a low-frequency signal. By eliminating the high-frequency

portion of the spectrum and performing an inverse Fourier transform, it is possible to obtain the original data with much of the noise removed.

Five additional parameters were required to fit the pyrrhotite and troilite spectra. The parameter YONE was needed to scale the calculated channel counts to those of the experimental spectrum. A1 and A2 were used to adjust inner line intensities affected by the finite depth of the sample. GX and GY were used to adjust inner line positions for second order effects (e.g., off diagonal magnetic and quadrupole terms). Each six-line multiplet was independently assigned the five parameters INT, WID, ISO, QUAD, and MAG; YONE, A1, A2, GY, and GX were parameters which applied to the entire spectrum and therefore represent averages.

MOSFIT contains a folding routine that is used to sum and average the data point of corresponding velocity as described previously. Using a PC computer, the data can be folded before they are transferred to the main frame. If the data is folded before it is sent to the main frame, the MOSFIT folding routine is skipped. MOSFIT also contains a digital filtering routine. This routine is used to lower the noise level in the spectra. Normally this value is set at a small value such as 1 or 2. If the spectra have a small amount of noise, the digital filter is set at zero. After MOSFIT passes through these two routines, it calculates the velocity scale from $-V_{max}$ to V_{max} for each channel. The spectra can now be plotted as absorption versus velocity. Using this type of plot, a subroutine is used to calculate a theoretical Lorentzian curve which describes the data.

Particle sizes

The magnetic properties of ferro-, ferri-, and antiferromagnetic materials consisting of very small sized particles (of a few tens of Angstroms) are quite different from those of bulk samples. Although each individual particle is in a magnetically ordered state, the whole system behaves as if it were paramagnetic. This is known

as superparamagnetism. Room temperature Mössbauer spectra of such systems do not exhibit hyperfine splittings. Lowering the temperature of the sample lengthens relaxation times and allows the system to magnetically order. Hyperfine splitting is then observed.

The average lifetime, τ, of a given state can be written:

$$\tau = exp\,(KV/k_BT)$$

where: K = magnetocrystalline anisotrophy energy constant (J/m^{-3}),

T = temperature (K),

V = volume of the magnetic particle (cm^{-3}), and

k_B = Boltzmann Constant.

The pre-exponential factor is also a function of the anisotrophy energy constant and the temperature. Thus, if the value of (τ) can be obtained, then it is possible to find KV can be deduced from the shape of Mössbauer spectra. Determinations of these parameters lead to particle size estimates (Morup et al. 1980).

In practice, a sample of small particles always contains a distribution of particle sizes, and the experimental spectra will then consist of a sum of spectra with different relaxation times. τ is very sensitive to the volume, and the distribution in relaxation times will be very broad. This implies that in many cases only a small fraction of the particles have relaxation times in the critical region (10^{-9} - 10^{-8} s), and the spectra can be described as consisting of a magnetically split component and a paramagnetic component. In general, the presence of a particle size distribution complicates the analysis, requiring that the observed Mössbauer spectrum be deconvoluted into its contributions from the different particles in the size distribution. Theory (Sharon and Tsuei 1972, Phillips et al. 1985) suggests that modes of collective magnetic excitation will result in a reduced hyperfine splitting for magnetic microcrystals held

below their blocking temperatures. This phenomenon has been used to determine approximate particle sizes using the formula:

$$\frac{measured\ splitting}{bulk\ splitting} = 1 - k_B T/2KV$$

where the measured and bulk hyperfine splittings are observed at temperature T. In the char experiments reported, liquid helium temperature is considered to be below the blocking temperatures of the samples.

A problem common for particle size determination is the estimation of the anisotropy energy parameter K. The determination of particle size using magnetic relaxations is thus coupled to a knowledge of KV; this is reminiscent of the way that selective chemisorption techniques of surface area measurements are related to the chemisorption stoichiometry. That is, the particle size can be estimated without an accurate knowledge of K since the magnitude of K can be estimated by involving physical arguments; relative changes in the particle size can be determined by experimental calibration, perhaps providing information in addition to that dealing with particle size. The methods of determining particle size distributions contained in superparamagnetic systems are well known and firmly established. While detailed and tedious, the techniques are straightforward (Williams et al. 1978, Christensen et al. 1985).

RESULTS AND DISCUSSION

Parameter values determined in the analysis of the spectra for all of the iron sulfides prepared in this study are tabulated in the Appendix. Spectra are also presented in the Appendix. Preparations identified as inflection point species were prepared by halting the reduction of pyrite at times corresponding to rate changes, and are considered to be pure phases. Preparations identified as intermediate, or

mid-point species, were prepared by halting the reactions at other times. They are mixtures of inflection point species.

The inflection point compositions are the iron sulfide standards used in this study. They are reliably unique. Independent preparations of these compositions have the same Mössbauer spectra. The spectrum of a phase tentatively identified as Machinawite has been obtained in this study and is discussed later in this section.

Parameter correlations were examined by plotting the average values of the isomer shifts, the quadrupole couplings, and the magnetic splittings versus the compositions of the species. In these plots only the inflection point (pure phases) spectra are used to determine the relationships.

Figure 1 is a plot of the average internal magnetic field versus pyrrhotite composition (atomic %Fe). Average fields are calculated by the form :

$$\{MAG\}_{average} = (n\{MAG\}_A + m\{MAG\}_B + 1\{MAG\}_C + k\{MAG\}_D)/(n+m+l+k),$$

where $\{MAG\}_A$, $\{MAG\}_B$, $\{MAG\}_C$, and $\{MAG\}_D$ are the respective magnetic splittings of sites A, B, C, and D; and n, m, l, and k are the respective spectral areas. These values are listed in the Appendix. In the plot, average fields for the inflection point species are plotted as filled squares and lie along a straight line described by

$$(MAG) = -408.2776 + (14.43992)(\%Fe).$$

Average fields derived from spectra of intermediate compositions are plotted in two ways. First, the average field calculated from the analysis of the spectra as mixtures of inflection point species are plotted on the graph as open squares, and also lie along the straight line. Average fields calculated for these same spectra fitted with the minimum number of Lorentzian multiplets, are plotted as crosses.

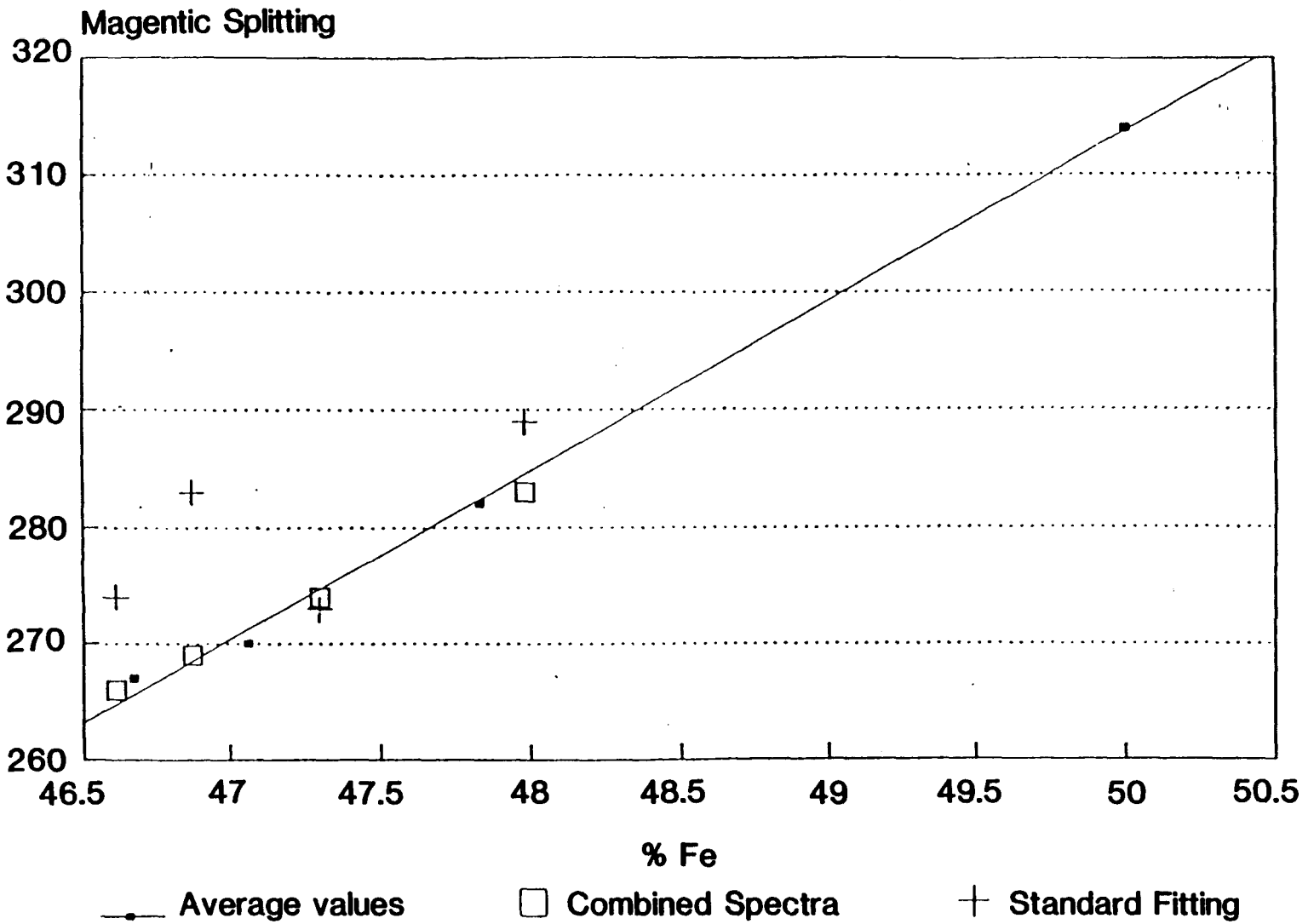

Figure 1. Average internal magnetic field versus pyrrhotite composition (atomic %Fe).

Plots obtained from the average value curves were used to indicate which of the fits for the mid-point spectra describes the data point more accurately. The results of the average value plots for the inflection point spectra indicate that the average values of internal magnetic field can be used as indices for the compositions of pure pyrrhotite phases. The average value of internal magnetic field is a reliable indicator of composition. Interpretations based upon mixtures of inflection point species for the spectra of intermediate compositions also follow this straight line, which indicates that these samples are mixtures and not separate pyrrhotites. Fittings of spectra of intermediate compositions with a minimum number of six-line multiplets do not yield average internal fields which are consistent with pure phases.

Figure 2 is a plot of isomer shifts as a function of iron composition (%Fe) for the inflection point species. Average values are listed in the Appendix. This plot shows that the isomer shift has a nonlinear relationship with the composition of the pyrrhotites.

Figure 3 is a plot of the average quadrupole coupling constants derived from the spectra of inflection point compositions versus iron composition (%Fe). These values are tabulated in the Appendix. This plot indicates that the quadrupole coupling also exhibits a nonlinear relationship with respect to composition. The relationship between the average quadrupole coupling constant and the composition of the inflection point compound exhibits a maximum for the composition Fe_8S_9.

Relationships among the parameters were studied by plotting the parameters against one another. In this way, it was possible to estimate correlations among the parameters. Figure 4 is a plot of the magnetic field versus isomer shift for the inflection point spectra. From this plot, it is shown that the isomer shift increases as the magnetic field increases from composition to composition. The relationship between the average isomer shift and the magnetic splitting is nonlinear.

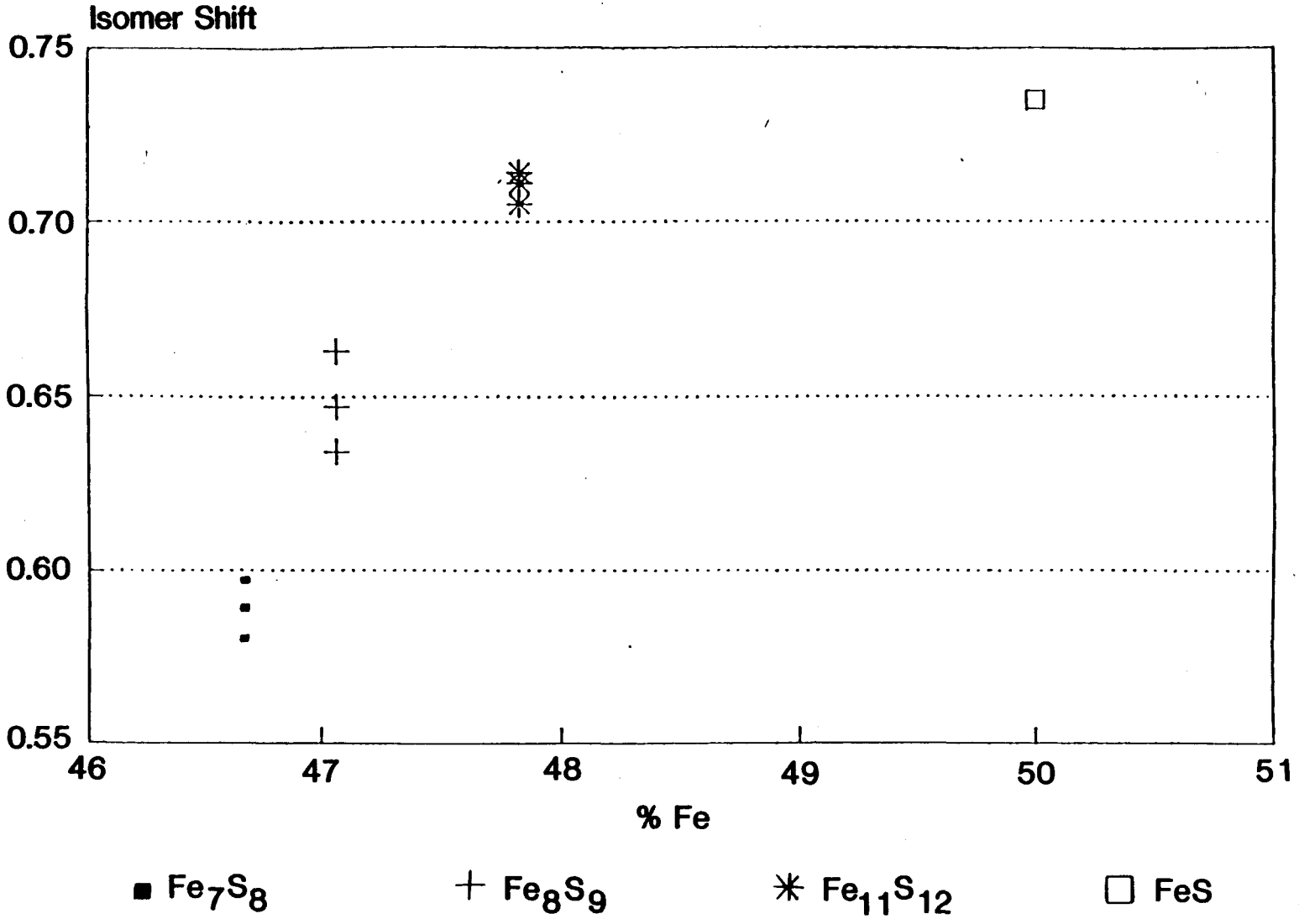

Figure 2. Isomer shifts as a function of iron composition (%Fe) for the inflection point species.

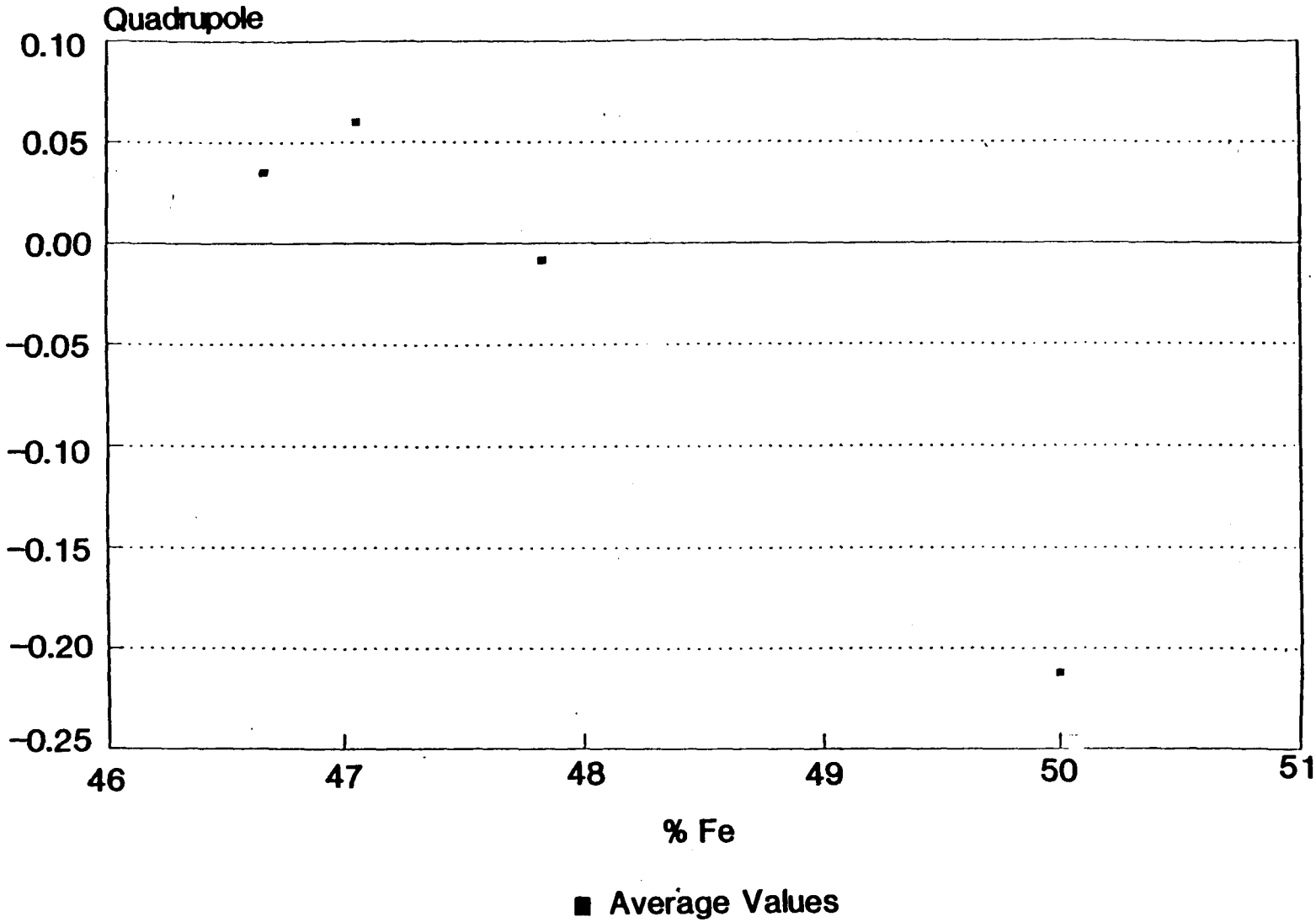

Figure 3. Average quadrupole coupling constants derived from the spectra of inflection point compositions versus iron composition (%Fe).

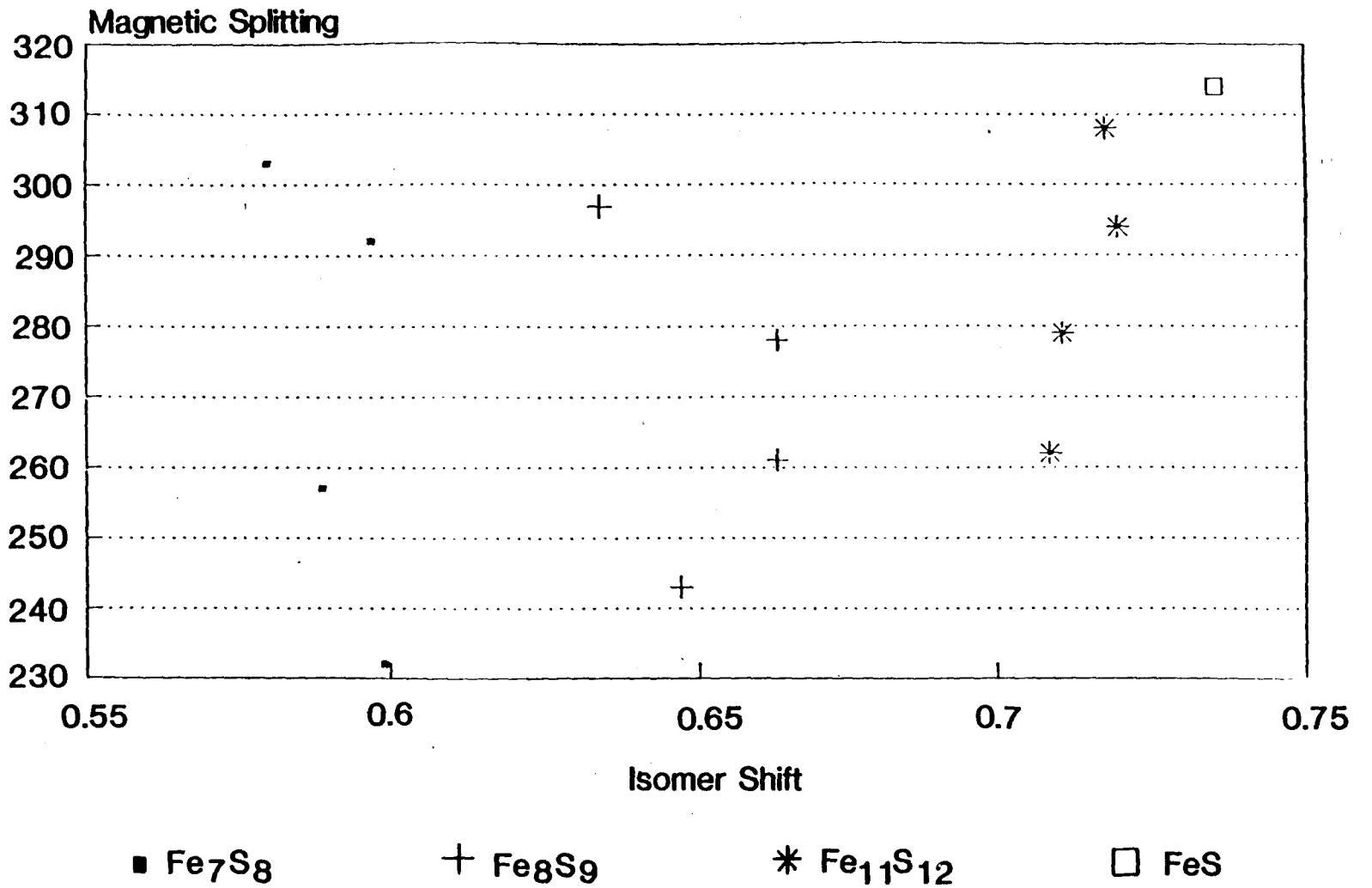

Figure 4. Magnetic field versus isomer shift for the inflection point spectra.

Figure 5 is a plot of quadrupole coupling versus isomer shift. In these materials, quadrupole coupling decreases as the isomer shift increases.

When the parameters are plotted against each other, trends in the data are observed that have not been observed previously. In the plot of magnetic splitting versus isomer shift, two types of trends can be seen. The first trend is that the isomer shift values increase as the magnetic splitting values increase for compositions. The trend in the parameters as reduction passes through the inflection point spectra tends to become more organized; for example the composition of $Fe_{11}S_{12}$ is more linear then the composition of Fe_7S_8. This same type of observation is observed for the plot of the quadrupole coupling versus isomer shift.

The spectrum of troilite, FeS, contains only one six-line multiplet. When pyrite is reduced past troilite by H_2, the spectrum becomes more complex. Additional six-line multiplets appear. One of the additional six-line multiplets has parameters normally associated with metallic iron. The other has parameters similar to a pyrrhotite. The magnetic splitting value is 296. The isomer shift value is between 0.620 and 0.700. The quadrupole coupling constant is between -0.4496 and -0.200.

A reduced troilite sample was prepared that contained only troilite and the second iron sulfide. No iron was present in this reduction. This indicates that the reaction of H_2 with FeS produces H_2S first and metallic iron second. This suggests that the second sulfide is a sulfur-deficient structure. These structures are tentatively identified as Machinawite.

Mössbauer spectroscopy was used to study superparamagnetic samples. In such a sample, for a given particle size, the Mössbauer spectra are Zeeman split when measured below the blocking temperature, while typical paramagnetic spectra with one or two lines are obtained considerably above this blocking temperature.

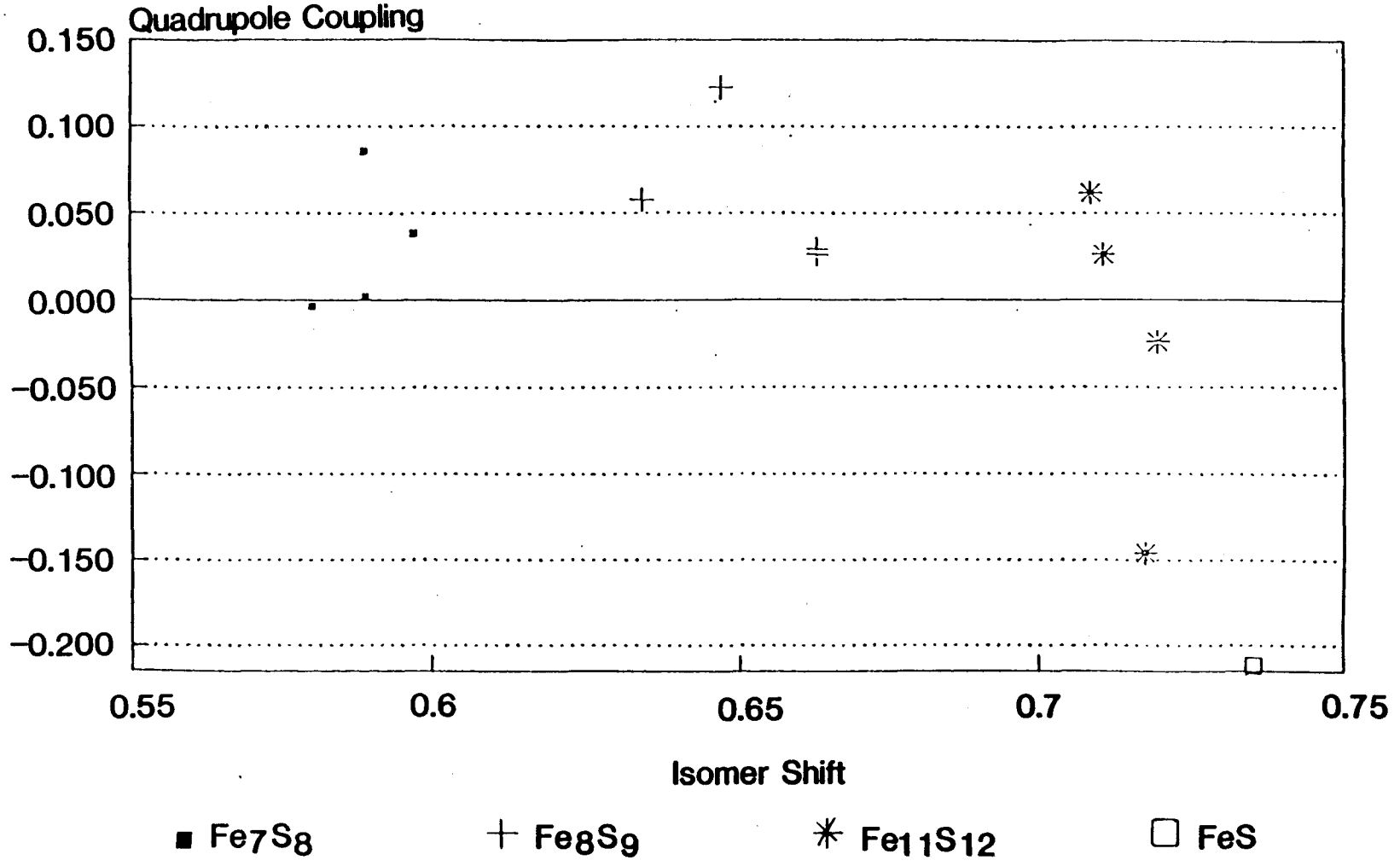

Figure 5. Quadrupole coupling versus isomer shift.

A standard sample of iron oxide was studied at room and liquid helium temperatures. The spectrum taken at 4.3K, composed of broadened sextuplets with asymmetric lines, was analyzed in terms of a hyperfine field distribution. A curve showing the field probability distribution P(H) is presented in Figure 6. It exhibits a sharp maximum at H_m = 485 kOe.

The particle size distribution for the standard oxide was calculated using the equivalent P(H) curve and the following procedure:

1. The range of diameters expected is divided into equal steps of length s, with an extremal value of d_{ex}.
2. For each d_{ex} the value of a is calculated from $a = Kd^3/6kT$, using $K = 1.0 \times 10^3$ Jm^{-3}.
3. The field H_{ex} corresponding to each d_{ex} is determined numerically using the following formula:

$$H_{ex} = H_L \frac{1}{2a^{1/2}} \frac{1 - exp(-a)}{F(a^{1/2})}$$

where $F(a^{1/2})$ is the Dawson integral.

4. Next the area under P(H) is calculated for each range H_{ex}. This area gives the probability P(d) of finding a diameter d (Figure 7).
5. Finally P(d) is normalized in such a way that P(d) = 10.

Thirteen acid-washed chars have been studied at room temperature. Five of these chars have been studied at 4.3K. Spectra obtained at 4.3K for three of these are presented in the Appendix, together with P(H) plots. For two of these samples, He992-15 and He992-22, P(H) plots indicate concentrations of species having internal magnetic fields consistent with pyrrhotites (e.g., 250 to 300 KOe). The third example exhibits only low concentrations of magnetically split absorptions.

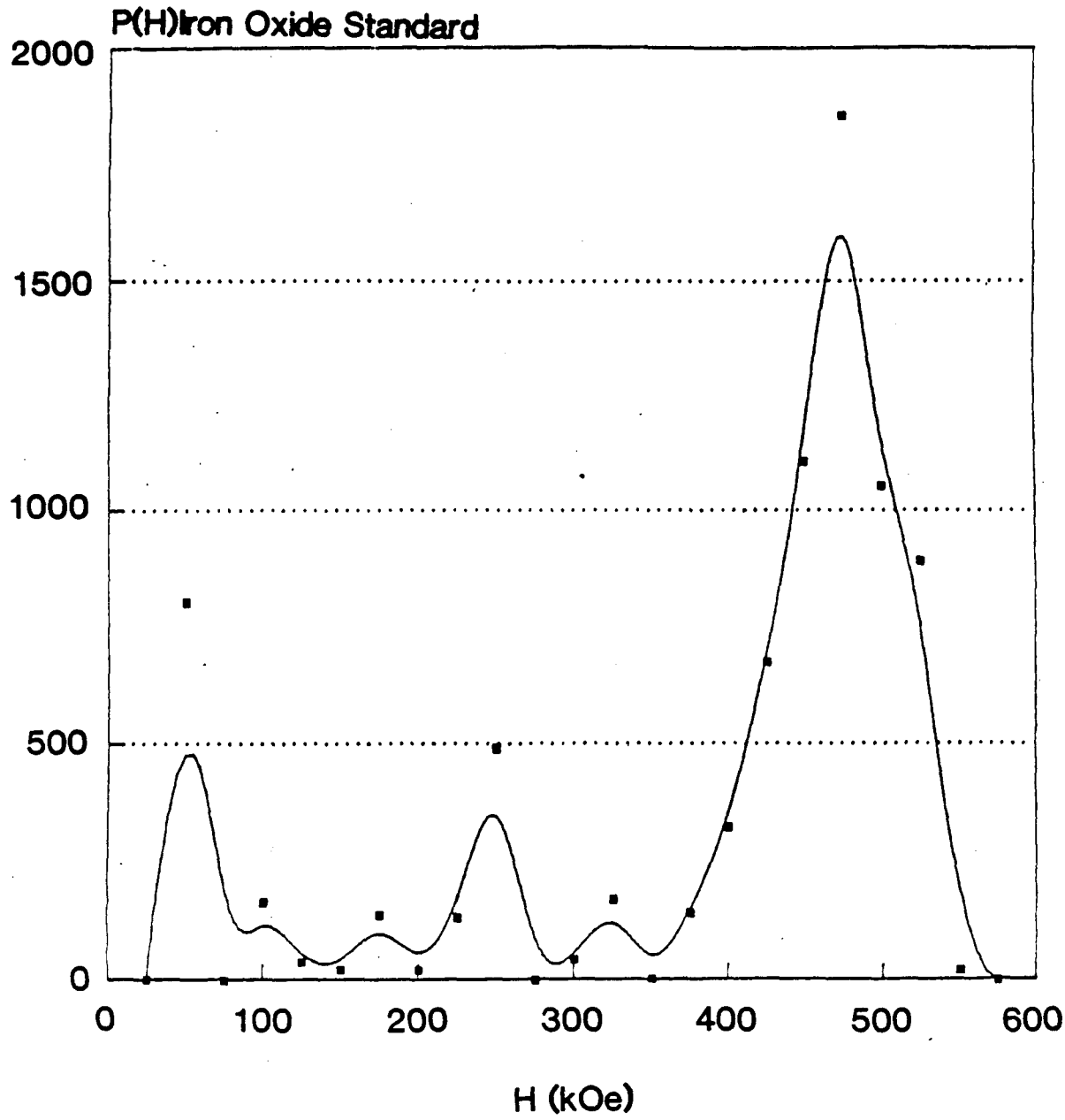

Figure 6. Field probability distribution.

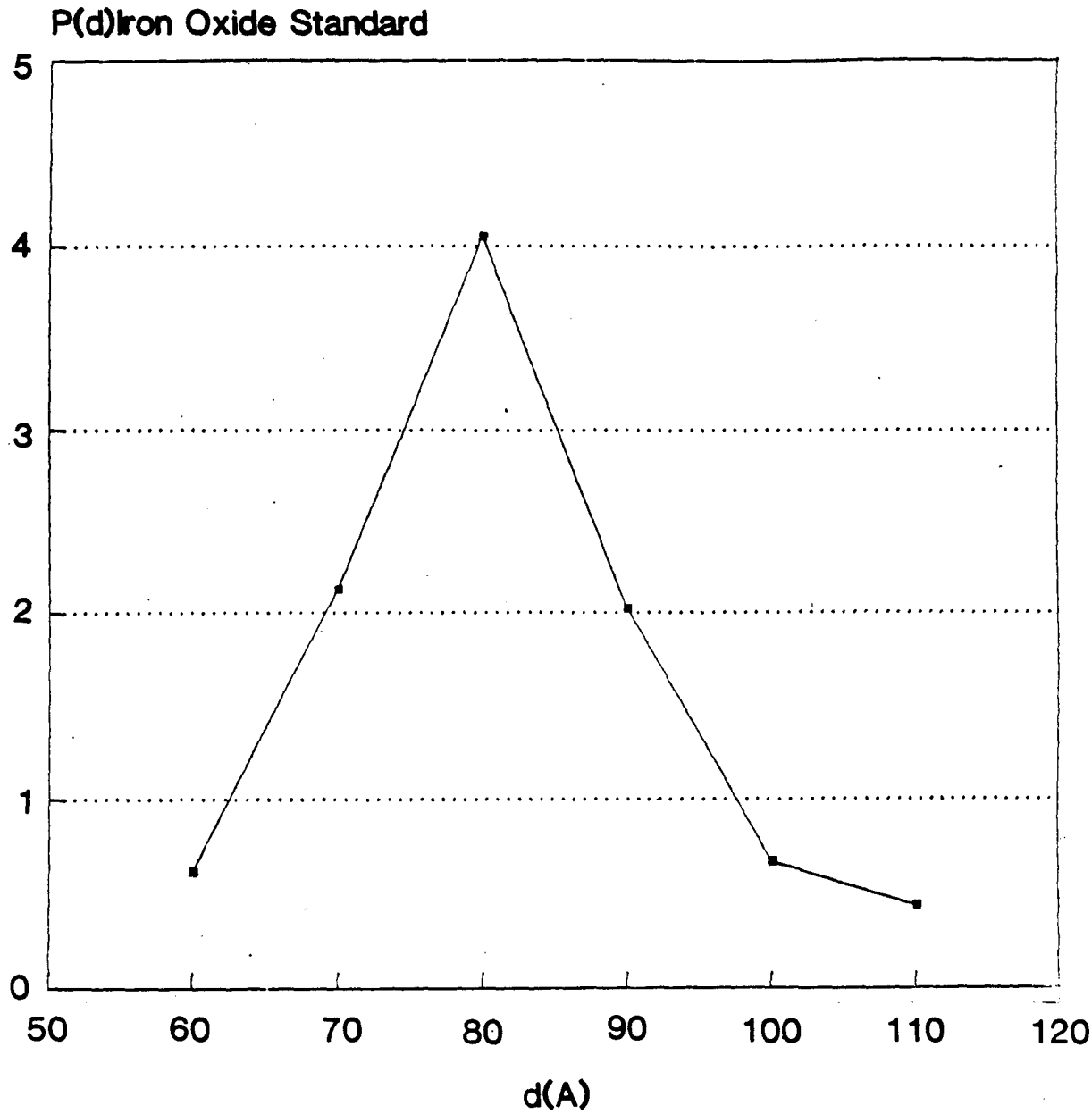

Figure 7. Probability P(d) of finding a diameter d.

These examples are typical. While part of the Mössbauer absorptions observed for these acid-washed chars can be attributed to iron sulfides, most of the absorptions are due to superparamagnetic iron oxides or to nonmagnetic iron compounds. This indicates that the vast majority of the pyrrhotite/troilite mixtures present in the desulfurized chars are accessible to the acid. Iron sulfide remaining after the acid wash is superparamagnetic. This material may be derived from microcrystalline pyrite present in the coal before the desulfurization treatment.

SUMMARY

The Mössbauer study confirms that the inflection point pyrrhotites are unique. Spectra of separate preparations are consistent.

The average magnetic splitting values are a good index of composition for the various pyrrhotites.

Internal magnetic fields, isomer shifts, and quadrupole coupling constants determined for the pure iron sulfides (inflection point species) correlate smoothly with iron sulfide composition.

The presence of a new iron sulfide in the reduction of troilite suggests the existence of a sulfur-deficient phase assigned as Machinawite.

Low-temperature spectra of several acid-washed chars have been obtained. The analyses are complicated by the low concentration of iron present in the chars. Nevertheless, it has been determined that about half of the chars contain microcrystalline particles, mostly of iron oxides. Some microcrystalline pyrrhotite is present.

REFERENCES

Aubanel, E., and K. Oldham. 1985. Fourier smoothing. Byte, February.

Christensen, P., S. Morup, W. Jahannes, and W. Niemantsverdriet. 1985. Particle size determination of supermagnetic -fe in carbon-supported catalysts by in situ Mössbauer spectroscopy. Journal of Physical Chemistry 89:4900-4903.

Kundig, W., R. Bommel, G. Constabalis, and R. Lindquist. 1966. Some properties of supported small $Fe_2 O_3$ particles determined with the Mössbauer effect. Physics Rev. 142(2):327-333.

Morup, S., J. Dumesic, and H. Topsoe. 1980. Magnetic microcrystals. In Applications of Mössbauer Spectroscopy. Academic Press.

Mukoyama, T., and H. Vegh. 1980. A new non-iterative method for fitting Lorentzian to Mössbauer spectra. Nuclear Inst. & Meth. 173:345-346.

Phillips, J., Y.Chen, and J. Dumesic. 1985. Characterization of supported iron oxide particles using Mössbauer spectroscopy and magnetic susceptibility. In Catalyst Characterization Science, pp. 518-533.

Sharon, T., and C. Tsuei. 1972. Magnetism in amorphous Fe-Pd-P alloys. Physics Rev. B 5(3):1047-1064.

Webster, J. R., R. H. Shiley, R. E. Hughes, P. L. Lapish, D. K. Cowin, G. V. Smith, C. C. Hinckley, T. Nishizawa, N. Yoshida, T. Wiltowski, Y. Wada, and M. Saporoschenko. 1985. Desulfurization of Illinois coal by in situ preparation of iron sulfide catalysts. In Proceedings of the Second Annual Pittsburgh Coal Conference. 16 September, Pittsburgh, PA. p. 138.

Williams, J., D. Danson, and C. Janot. 1978. A Mössbauer determination of the iron core particle size distribution in Ferritin. Phys. Med. Biol. 23(5):835-351.

Wiltowski, T., C. C. Hinckley, G. V. Smith, T. Nishizawa, M. Saporoschenko, R. H. Shiley, and J. R. Webster. 1987. Kinetics and mechanism of iron sulfide reduction in hydrogen and in carbon monoxide. Journal of Solid State Chemistry 71:95-102.

Winkler, W. 1984. Mössbauer studies of small magnetic particles of a magnetic fluid. Phys. Stat. Sol. 84(a):193-198.

Zimmerman, E. 1981. Guide to spectral analysis. 1981. Byte, February.

APPENDIX

Section 1. Mössbauer parameters of iron sulfides.

Section 2. Mössbauer spectra of pure iron sulfides.

Section 3. Mössbauer spectra of reduced troilite.

Section 4. Selected Mössbauer of mixed iron sulfide phases.

Section 5. Selected low temperature Mössbauer spectra of acid-washed desulfurized coal chars, with P(H) distribution plots.

Section 6. Mössbauer spectra of acid-washed desulfurized coal chars.

Appendix: Section 1

TABLE I

PARAMETERS FOR PYRITE AND TROILITE

Assignment	INT	WID	ISO	QUAD	MAG	CONC
FeS_2 (%Fe=33.33)						
Pyrite	.0586	0.437	0.350	0.763		
FeS (%Fe=50)						
Troilite	.00825	0.232	0.735	-0.212	314	

TABLE II

PARAMETERS FOR THE SAMPLES REDUCED BY H_2

Assignment	INT	WID	ISO	QUAD	MAG	CONC
PYRITE2: FeS_2 reduced 2 hours						
Pyrrhotite	.00621	0.308	0.587	.0555	296	10.72
Pyrrhotite	.00668	0.545	0.585	.0413	253	20.39
Pyrite	.232	0.318	0.263	0.618		68.89
PYH26: $FeS_{1.578}$ (between FeS_2 and Fe_7S_8)						
Pyrrhotite	.00346	0.416	0.729	.0704	305	20.84
Pyrrhotite	.00129	0.239	0.721	.0317	284	4.47
Pyrrhotite	.00286	0.359	0.706	.0687	263	14.87
Pyrrhotite	.00228	0.467	0.702	.0250	240	15.42
Pyrite	.02715	0.678	0.438	0.542		44.42
PYRIT3: FeS_8S_9 (%Fe=47.06)						
Pyrrhotite	.00503	0.230	0.580	-.0035	303	12.52
Pyrrhotite	.00661	0.319	0.597	.0382	292	22.82
Pyrrhotite	.00838	0.361	0.589	.0020	257	32.75
Pyrrhotite	.00518	0.339	0.589	.0855	232	19.01
Pyrite	.02849	0.251	0.319	0.596		12.90
PYH29: Reduced past Fe_7S_8 and before Fe_8S_9						
Pyrrhotite	.00021	0.623	0.616	.0314	308	11.87
Pyrrhotite	.00097	0.577	0.724	-.0105	291	50.77
Pyrrhotite	.00057	0.528	0.697	0.110	265	27.30
Pyrrhotite	.00029	0.248	0.512	0.116	238	6.52
Pyrite	.00062	0.377	0.308	0.602		3.53
PYRITE4: Fe_7S_8 (%Fe=46.67)						
Pyrrhotite	.00697	0.301	0.634	.0575	297	27.50
Pyrrhotite	.00432	0.305	0.663	0.265	278	17.27
Pyrrhotite	.00679	0.314	0.663	.0290	261	27.87
Pyrrhotite	.00434	0.410	0.647	0.124	243	23.33
Pyrite	.00801	0.230	0.298	0.608		4.03

CONTINUED NEXT PAGE

TABLE II CONTINUED

Assignment	INT	WID	ISO	QUAD	MAG	CONC
PYH25: $FeS_{1.12}$ (between Fe_8S_9 and $Fe_{11}S_{12}$)						
Pyrrhotite	.00042	0.368	0.637	-.0046	309	12.90
Pyrrhotite	.00065	0.527	0.709	0.128	290	28.60
Pyrrhotite	.00085	0.426	0.677	0.148	260	30.23
Pyrrhotite	.00039	0.494	0.650	0.195	235	16.09
Pyrite	.00168	0.521	0.350	0.656		12.18
PYRITE5: $Fe_{11}S_{12}$ (%Fe=47.83)						
Pyrrhotite	.00434	0.243	0.714	-0.146	308	19.60
Pyrrhotite	.00556	0.292	0.705	.0610	262	30.18
Pyrrhotite	.00568	0.283	0.711	.0228	278	29.77
Pyrrhotite	.00406	0.269	0.714	-.0249	293	20.45
PYH24: $FeS_{1.047}$ (between $Fe_{11}S_{12}$ and FeS)						
Pyrrhotite	.00263	0.472	0.736	-0.152	310	33.34
Pyrrhotite	.00297	0.480	0.720	.0246	291	38.29
Pyrrhotite	.00174	0.322	0.735	.0787	272	15.05
Pyrrhotite	.00146	0.340	0.725	0.152	253	13.33
TOMEKA1: Pyrite redued past troilite						
Iron	.00293	0.289	0.032	0.188	341	21.42
Troilite	.00656	0.338	0.655	-0.238	312	56.10
Pyrrhotite	.00343	0.259	0.630	0.441	296	22.48
PYH30: Reduced Troilite						
Troilite	.00243	0.339	0.730	-0.124	314	76.36
Pyrrhotite	.00100	0.255	0.667	-0.235	295	23.64

TABLE III

PARAMETERS FOR THE SAMPLES REDUCED BY CO

Assignment	INT	WID	ISO	QUAD	MAG	CONC
RC03: $FeS_{1.032}$ (between FeS_2 and $Fe_{11}S_{12}$)						
Pyrrhotite	.00165	0.491	0.725	.0116	301	20.75
Pyrrhotite	.00226	0.459	0.736	.0950	280	26.56
Pyrrhotite	.00232	0.418	0.713	0.151	261	24.83
Pyrrhotite	.00143	0.419	0.706	0.179	239	15.34
Pyrite	.00826	0.355	0.251	0.587		12.52
RC05: $FeS_{1.13}$ (between FeS_2 and $Fe_{11}S_{12}$)						
Pyrrhotite	.00110	0.321	0.781	-0.235	321	9.01
Pyrrhotite	.00279	0.447	0.709	0.124	269	31.81
Pyrrhotite	.00288	0.449	0.734	.0518	288	32.81
Pyrrhotite	.00243	0.340	0.732	.0505	308	21.07
Pyrite	.00276	0.437	0.303	0.510		5.13
RC04: Reduced to $Fe_{11}S_{12}$						
Pyrrhotite	.00231	0.352	0.776	-0.248	321	17.86
Pyrrhotite	.00286	0.411	0.712	0.126	268	25.81
Pyrrhotite	.00319	0.417	0.747	.0286	287	29.21
Pyrrhotite	.00315	0.392	0.747	-.0011	308	27.12
RC06: Reduced between $Fe_{11}S_{12}$ and FeS						
Pyrrhotite	.00086	0.386	0.800	-0.152	314	38.72
Pyrrhotite	.00065	0.345	0.777	-.0037	272	26.16
Pyrrhotite	.00075	0.298	0.740	-.0513	293	26.07
Pyrrhotite	.00028	0.277	0.704	0.195	258	9.05

TABLE IV

PARAMETERS FOR THE INTERMEDIATE SPECTRA

Assignment	INT	WID	ISO	QUAD	MAG	CONC
PYRITE2: Fit using Fe_7S_8						
Pyrrhotite	.00389	0.300	0.580	-.0035	303	6.79
Pyrrhotite	.00436	0.274	0.597	.0383	292	6.95
Pyrrhotite	.00502	0.302	0.589	.0020	257	8.82
Pyrrhotite	.00292	0.353	0.589	.0855	232	6.00
Pyrite	.23310	0.316	0.263	0.616		71.44
PYH26: Fit using Fe_7S_8						
Pyrrhotite	.00152	0.230	0.580	-.0035	303	6.79
Pyrrhotite	.00251	0.391	0.597	.0383	292	6.95
Pyrrhotite	.00337	0.361	0.589	.0020	257	8.82
Pyrrhotite	.00205	0.339	0.589	.0855	232	6.00
Pyrite	.02610	0.452	0.263	0.616		71.44
PYH29: Fit using Fe_7S_8 and Fe_8S_9						
Percentage of Fe_7S_8 = 40%						
Pyrrhotite	.00503	0.230	0.580	-.0035	303	6.50
Pyrrhotite	.00661	0.319	0.597	.0382	292	10.04
Pyrrhotite	.00838	0.361	0.589	.0020	257	15.57
Pyrrhotite	.00518	0.339	0.589	.0855	232	9.03
Percentage of Fe_8S_9 = 60%						
Pyrrhotite	.00697	0.301	0.634	.0575	297	16.25
Pyrrhotite	.00432	0.305	0.663	0.265	278	10.19
Pyrrhotite	.00679	0.314	0.663	.0290	261	16.39
Pyrrhotite	.00434	0.410	0.647	0.124	243	13.79
Pyrite	.00062	0.377	0.308	0.602		2.25
PYH25: $FeS_{1.12}$ fit using $Fe_{1.17}S$ and $Fe_{11}S_{12}$						
Percentage of $FeS_{1.17}$ = 57%						
Pyrrhotite	.00697	0.301	0.634	.0575	297	19.73
Pyrrhotite	.00432	0.305	0.663	0.265	278	7.45
Pyrrhotite	.00679	0.314	0.663	.0290	261	15.82
Pyrrhotite	.00434	0.410	0.647	0.124	243	11.55

CONTINUED NEXT PAGE

TABLE IV CONTINUED

Assignment	INT	WID	ISO	QUAD	MAG	CONC
Percentage of $Fe_{11}S_{12}$ = 45.77						
Pyrrhotite	.00434	0.243	0.714	-0.146	308	7.10
Pyrrhotite	.00556	0.292	0.705	.0610	262	10.73
Pyrrhotite	.00568	0.283	0.711	.0228	278	12.42
Pyrrhotite	.00406	0.269	0.714	-.0249	293	6.65
Pyrite	.00168	0.521	0.350	0.656		8.54
PYH24: $FeS_{1.047}$ fit using $Fe_{11}S_{12}$ and FeS						
Percentage of $Fe_{11}S_{12}$ = 81%						
Pyrrhotite	.00434	0.243	0.714	-0.146	308	19.10
Pyrrhotite	.00556	0.292	0.705	.0610	262	29.37
Pyrrhotite	.00568	0.283	0.711	.0228	278	29.08
Pyrrhotite	.00406	0.269	0.714	-.0249	293	19.97
FeS Percentage = 15.88						
Troilite	.00825	0.232	0.735	-0.212	314	2.45
<u>REDUCTION BY CO</u>						
RC03: Fit using RC04 ($Fe_{11}S_{12}$)						
Pyrrhotite	.00029	0.352	0.776	-0.248	321	3.41
Pyrrhotite	.00298	0.411	0.712	0.126	268	40.91
Pyrrhotite	.00229	0.417	0.747	.0286	287	31.89
Pyrrhotite	.00053	0.392	0.747	-.0011	308	6.94
Pyrite	.00853	0.355	0.251	0.587		
RC05: Fit using RC04						
Pyrrhotite	.00188	0.352	0.776	-0.248	321	17.43
Pyrrhotite	.00234	0.411	0.712	0.126	268	25.41
Pyrrhotite	.00261	0.417	0.747	.0286	287	28.75
Pyrrhotite	.00251	0.392	0.747	-.0011	308	26.61
Pyrite	.00117	0.350	0.301	0.602		1.80

CONTINUED NEXT PAGE

TABLE IV CONTINUED

Assignment	INT	WID	ISO	QUAD	MAG	CONC
RC06: Fit using RC04 and FeS						
Percentage of $Fe_{11}S_{12}$ = 69%						
Pyrrhotite	.00231	0.352	0.776	-0.248	321	16.37
Pyrrhotite	.00286	0.411	0.712	0.126	268	23.83
Pyrrhotite	.00319	0.417	0.747	.0286	287	26.97
Pyrrhotite	.00315	0.392	0.747	-.0011	308	18.65
Percentage of FeS = 31%						
Troilite	.00825	0.232	0.735	-0.212	314	14.18

TABLE V

AVERAGE VALUES FOR THE MAGNETIC SPLITTING

Spectra reduced by H_2		Spectra reduced by CO	
Spectra	Ave. Mag. Field	Spectra	Ave. Mag. Field
PYRIT3	267		
PYRITE4	270		
PYRITE5	282	RCO4	294
TOMEK10	314	TOMEK10	314
	Intermediate spectra		
PYRITE2	267	RCO3	272
PYH26	274	RCO5	289
PYH29	283	RCO6	292
PYH25	273		
PYH24	289		
TOMEKA1	315		
PYH30	309		
	For combined inflection point spectra		
PYRITE2	271	RCO3	281
PYH26	266	RCO5	294
PYH29	269	RCO6	296
PYH25	274		
PYH24	283		

TABLE VI

AVERAGE VALUES FOR THE ISOMER SHIFT

Spectra reduced by H_2		Spectra reduced by CO	
Spectra	Ave. Isomer Shift	Spectra	Ave. Isomer Shift
PYRIT3	0.589		
PYRITE4	0.644		
PYRITE5	0.710	RCO4	0.740
TOMEK10	0.735	TOMEK10	0.735
	Intermediate spectra		
PYRITE2	0.585	RCO3	0.723
PYH26	0.715	RCO5	0.730
PYH29	0.689	RCO6	0.770
PYH25	0.677		
PYH24	0.728		
TOMEKA1	0.516		
PYH30	0.715		
	For combined inflection point spectra		
PYRITE2	0.589	RCO3	0.730
PYH26	0.590	RCO5	0.740
PYH29	0.621	RCO6	0.672
PYH25	0.631		
PYH24	0.711		

Appendix: Section 2

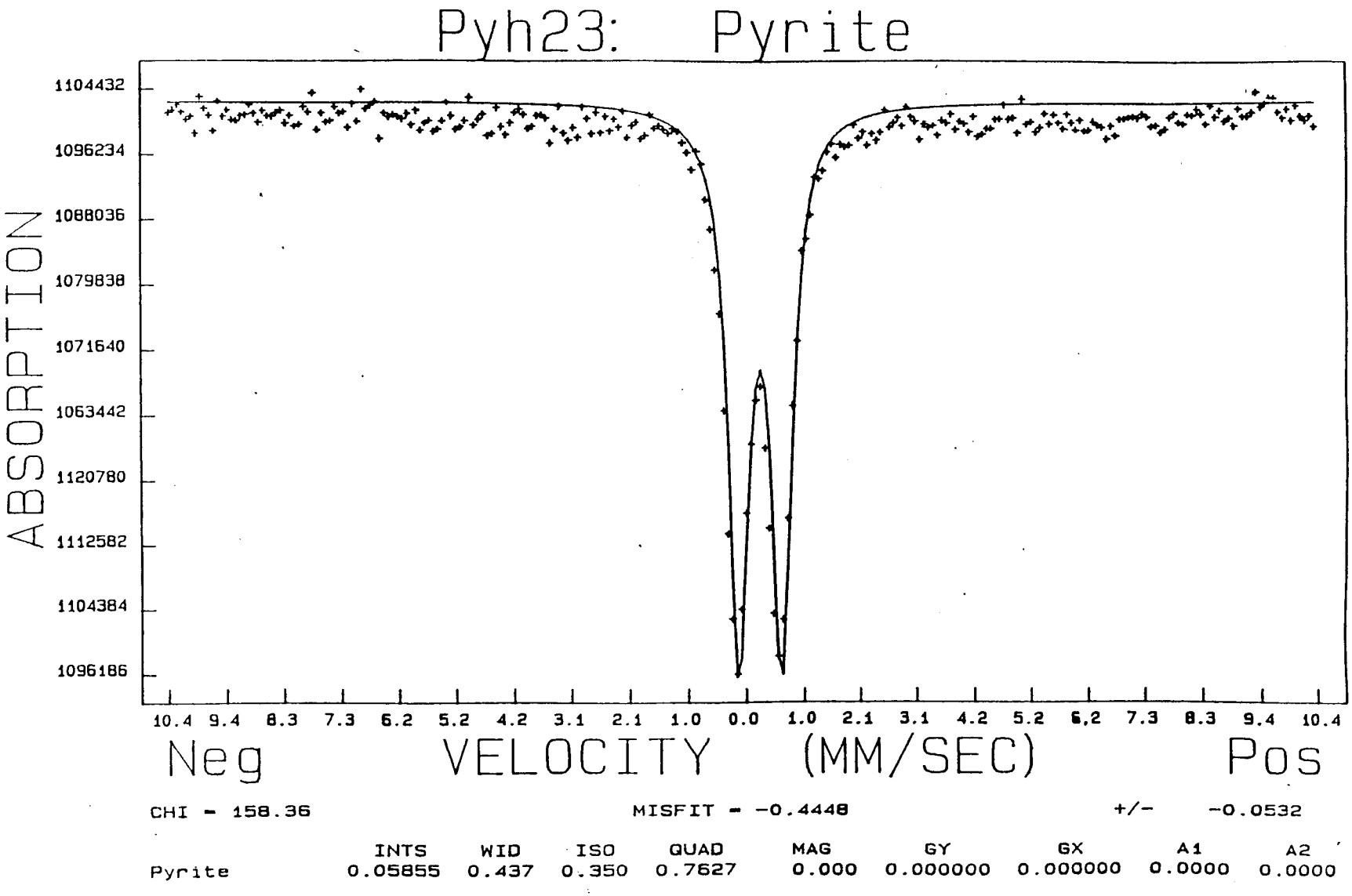
Pyh23: Pyrite
ABSORPTION
1104432
1096234
1088036
1079838
1071640
1063442
1120780
1112582
1104384
1096186
10.4 9.4 8.3 7.3 6.2 5.2 4.2 3.1 2.1 1.0 0.0 1.0 2.1 3.1 4.2 5.2 6.2 7.3 8.3 9.4 10.4
Neg VELOCITY (MM/SEC) Pos
CHI = 158.36
MISFIT = -0.4448
+/- -0.0532
INTS WID ISO QUAD MAG GY GX A1 A2
Pyrite 0.05855 0.437 0.350 0.7627 0.000 0.000000 0.000000 0.0000 0.0000

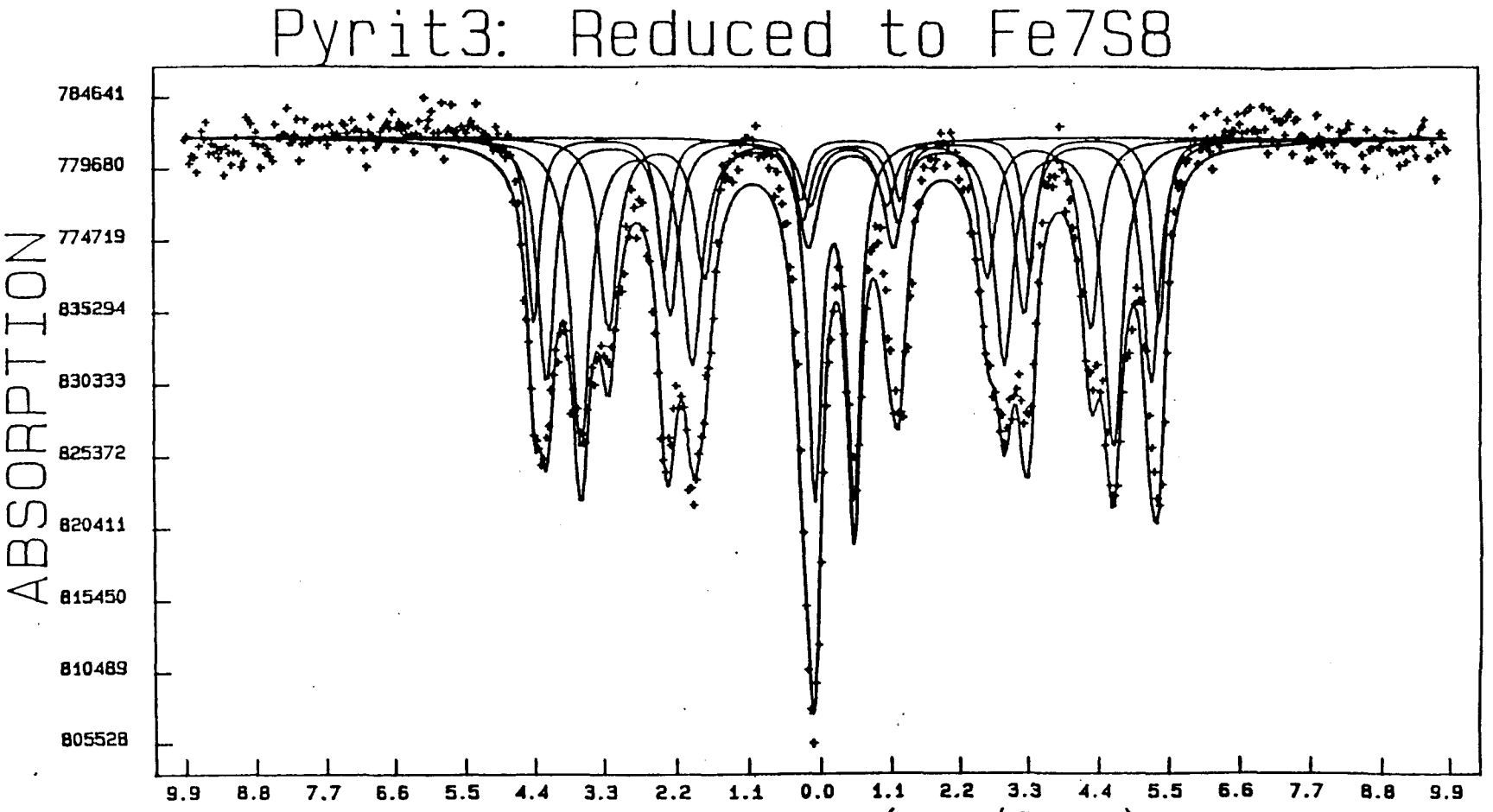

CHI = 1819.24 MISFIT = 1.7369 +/- 0.1015

	INTS	WID	ISO	QUAD	MAG	GY	GX	A1	A2
Pyrrhotite	0.00503	0.230	0.580	-0.0035	302.550	0.000091	-0.000004	0.1688	0.0206
Pyrrhotite	0.00661	0.319	0.597	0.0382	292.490	0.000091	-0.000004	0.1688	0.0206
Pyrrhotite	0.00838	0.361	0.589	0.0020	257.170	0.000091	-0.000004	0.1688	0.0206
Pyrrhotite	0.00518	0.339	0.589	0.0855	232.240	0.000091	-0.000004	0.1688	0.0206
Pyrite	0.02849	0.251	0.319	0.5961	0.000	0.000000	0.000000	0.0000	0.0000

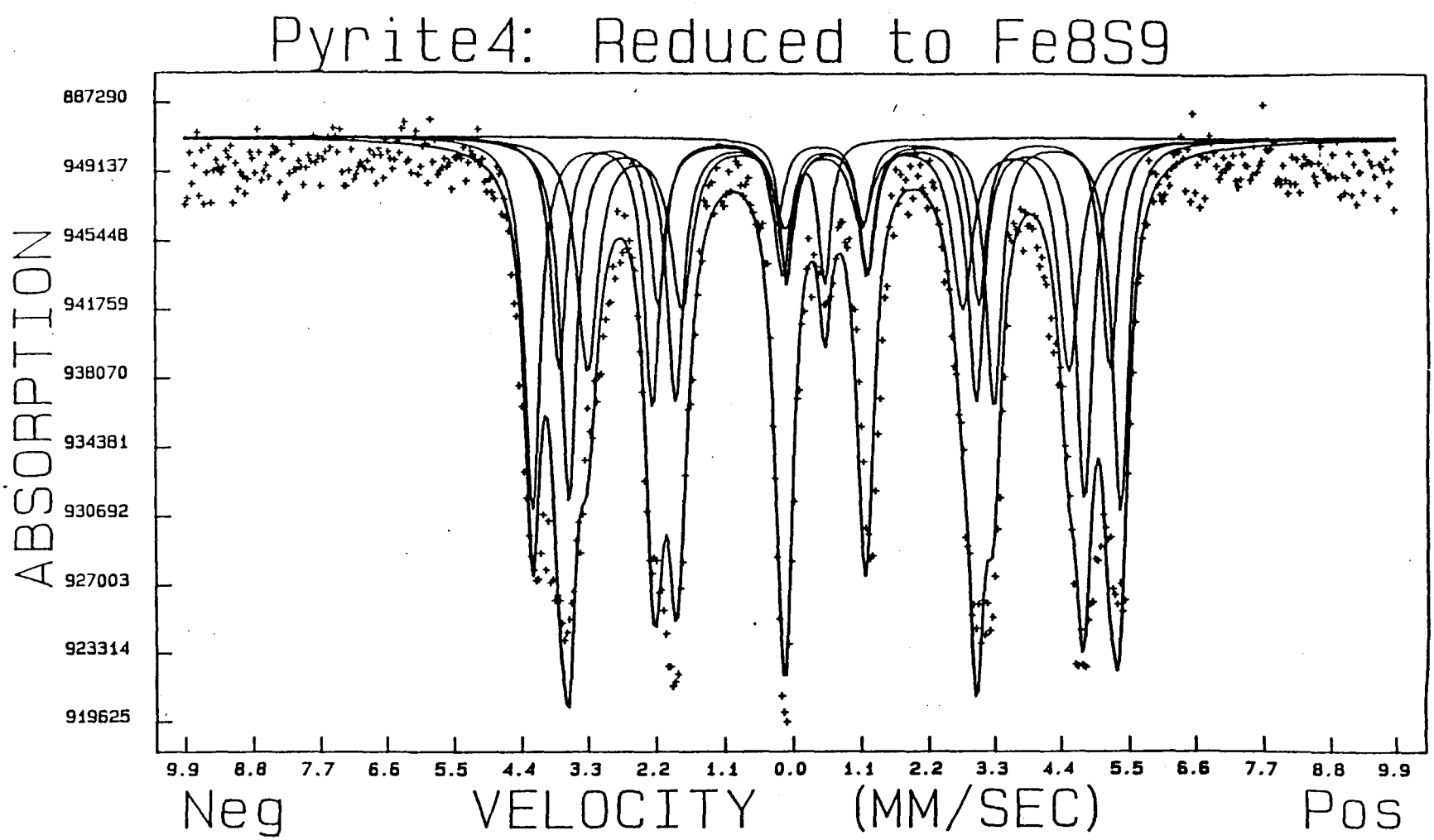

CHI = 1048.09 MISFIT = 0.7738 +/- 0.0746

	INTS	WID	ISO	QUAD	MAG	GY	GX	A1	A2
Pyrrhotite	0.00697	0.301	0.634	0.0575	297.010	-0.000003	-0.000269	0.1606	0.0937
Pyrrhotite	0.00432	0.305	0.663	0.2646	278.480	-0.000003	-0.000027	0.1606	0.0937
Pyrrhotite	0.00677	0.314	0.663	0.0290	260.860	-0.000003	-0.000027	0.1606	0.0937
Pyrrhotite	0.00434	0.410	0.647	0.1239	243.190	-0.000003	-0.000027	0.1606	0.0937
Pyrite	0.00801	0.230	0.298	0.6081	0.000	0.000000	0.000000	0.0000	0.0000

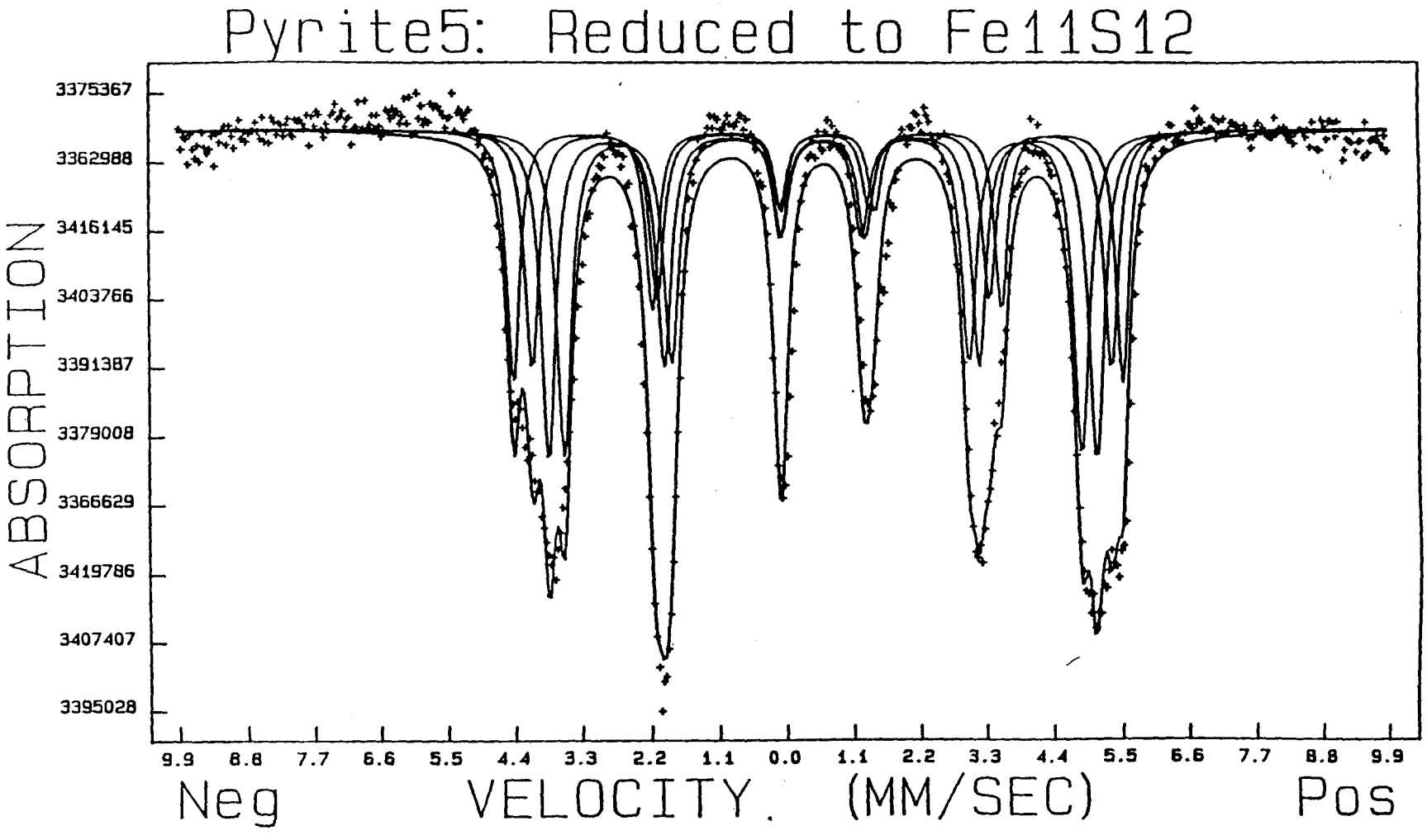

CHI = 2893.90 MISFIT = 1.5942 +/- 0.0676

	INTS	WID	ISO	QUAD	MAG	GY	GX	A1	A2
Pyrrhotite	0.00434	0.243	0.714	-0.1455	307.950	-0.000050	-0.000055	0.1294	-0.0405
Pyrrhotite	0.00556	0.292	0.705	0.0610	262.180	-0.000050	-0.000055	0.1294	-0.0405
Pyrrhotite	0.00566	0.283	0.711	0.0228	277.560	-0.000050	-0.000055	0.1294	-0.0405
Pyrrhotite	0.00409	0.269	0.714	-0.0249	293.080	-0.000050	-0.000055	0.1294	-0.0405

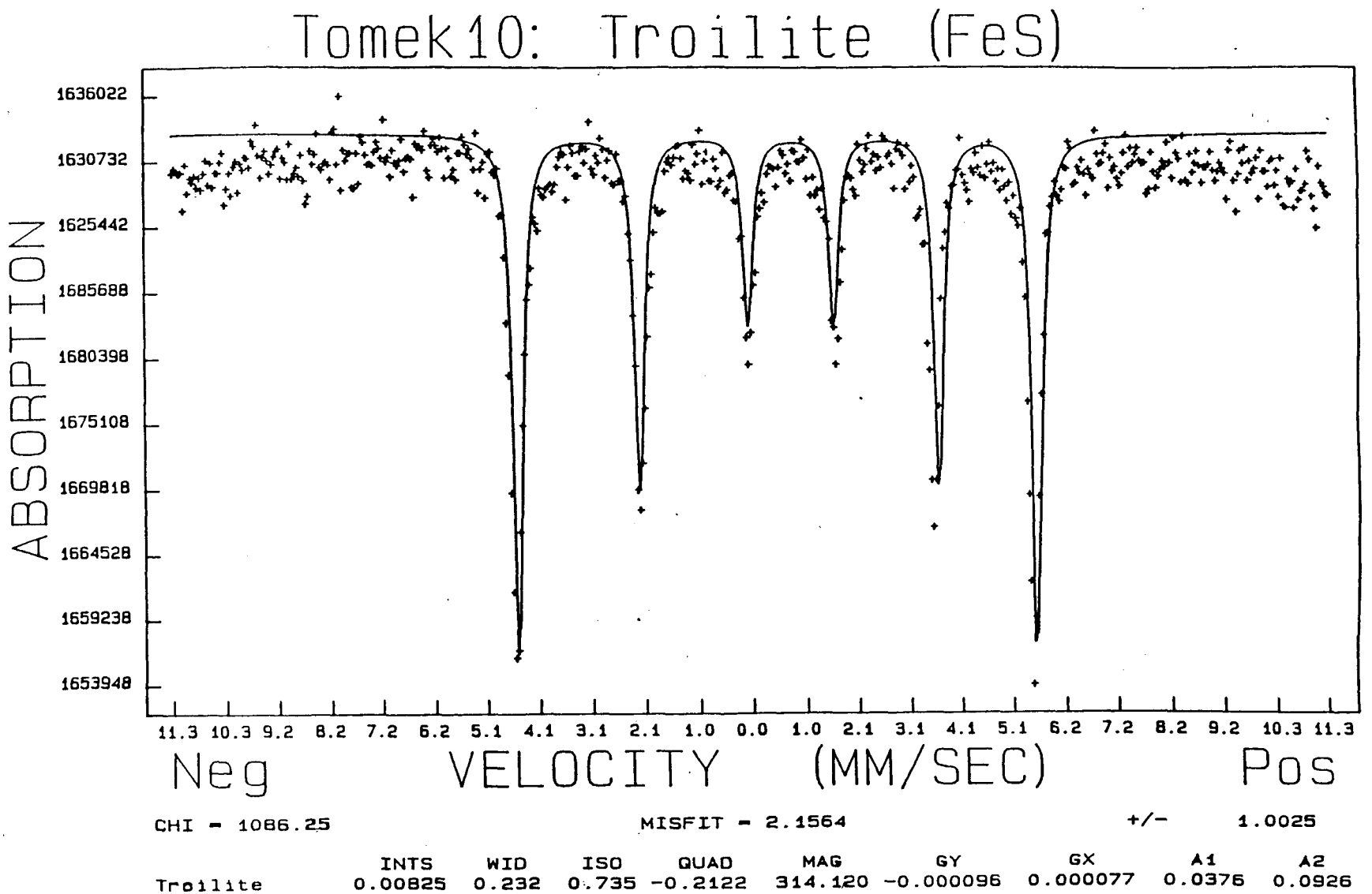
Tomek10: Troilite (FeS)
ABSORPTION
1636022
1630732
1625442
1685688
1680398
1675108
1669818
1664528
1659238
1653948
11.3 10.3 9.2 8.2 7.2 6.2 5.1 4.1 3.1 2.1 1.0 0.0 1.0 2.1 3.1 4.1 5.1 6.2 7.2 8.2 9.2 10.3 11.3
Neg VELOCITY (MM/SEC) Pos
CHI = 1086.25
MISFIT = 2.1564
+/- 1.0025
INTS WID ISO QUAD MAG GY GX A1 A2
Troilite 0.00825 0.232 0.735 -0.2122 314.120 -0.000096 0.000077 0.0376 0.0926

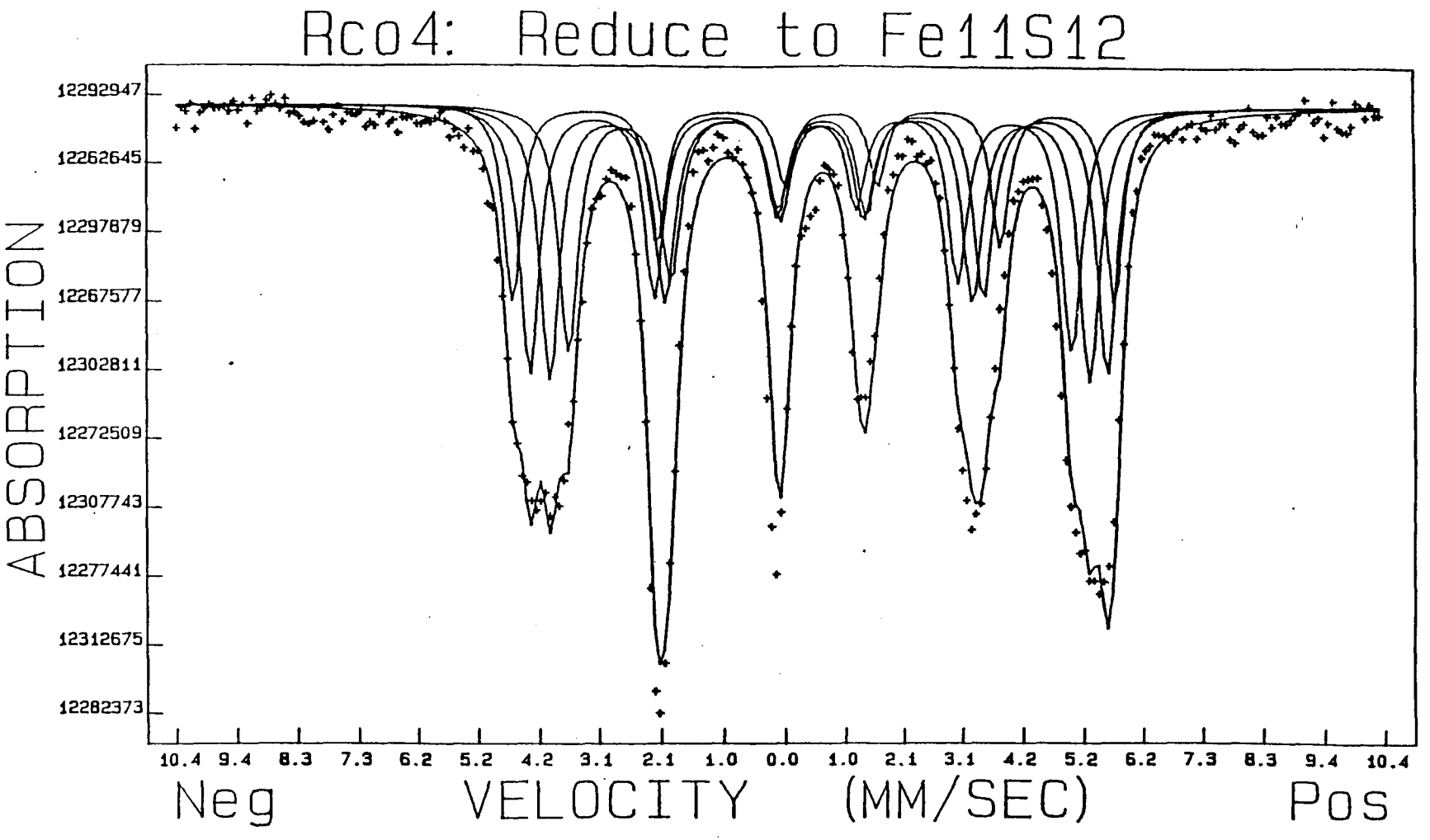

CHI = 456.01 MISFIT = 0.2710 +/- 0.0441

	INTS	WID	ISO	QUAD	MAG	GY	GX	A1	A2
Pyrrhotite	0.00231	0.352	0.776	-0.2476	320.520	-0.000108	-0.000028	0.1238	0.2170
Pyrrhotite	0.00286	0.411	0.712	0.1257	267.720	-0.000108	-0.000028	0.1238	0.2170
Pyrrhotite	0.00319	0.417	0.747	0.0286	287.350	-0.000108	-0.000029	0.1238	0.2170
Pyrrhotite	0.00315	0.392	0.736	-0.0011	307.570	-0.000108	-0.000028	0.1238	0.2170

Appendix: Section 3

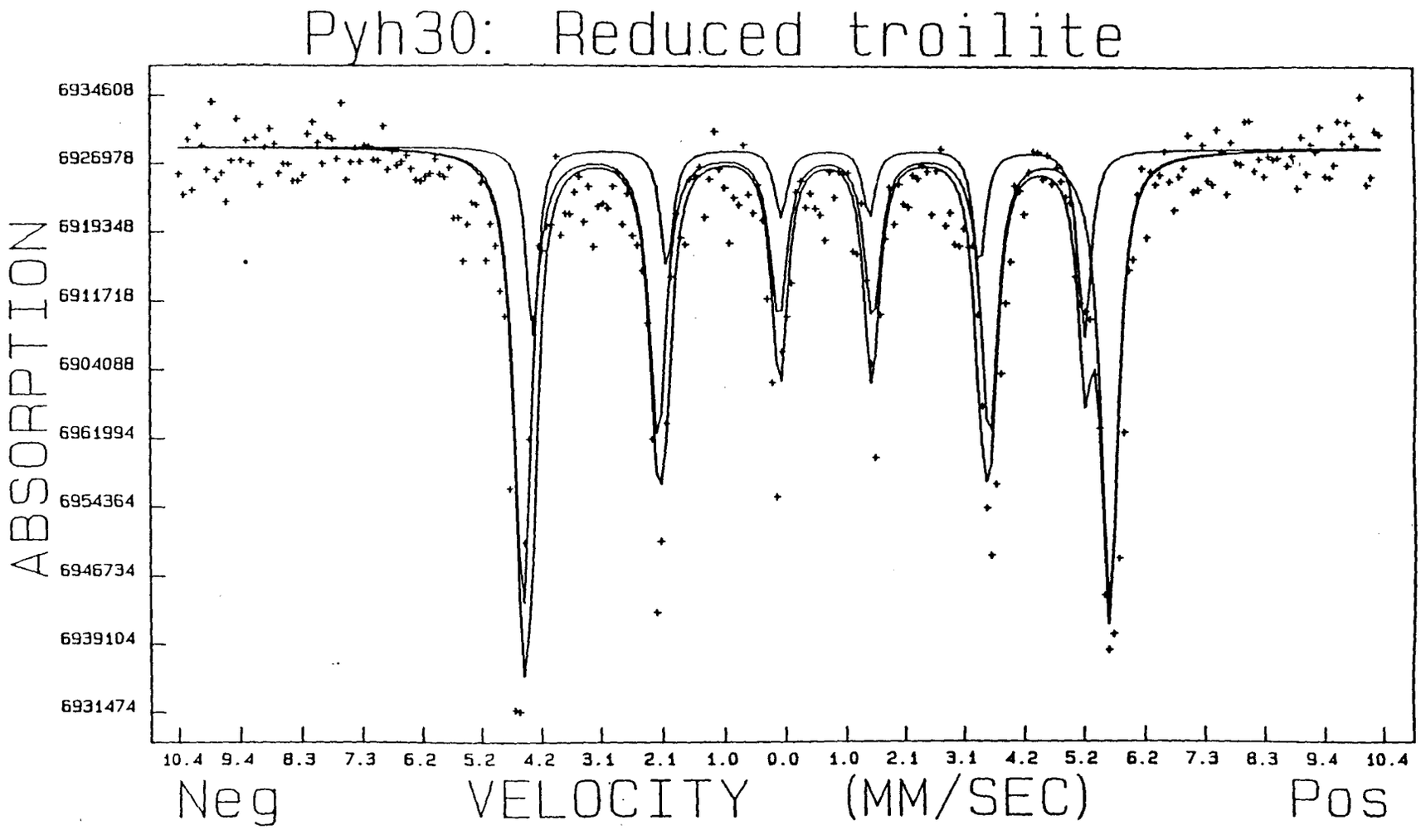

CHI = 606.04 MISFIT = 11.0300 +/- 1.3420

	INTS	WID	ISO	QUAD	MAG	GY	GX	A1	A2
Troilite	0.00243	0.339	0.730	-0.1236	313.530	-0.000217	0.000037	-0.1134	0.0976
Pyrrhotite	0.00100	0.255	0.667	-0.2350	295.310	-0.000217	0.000037	-0.1134	0.0976

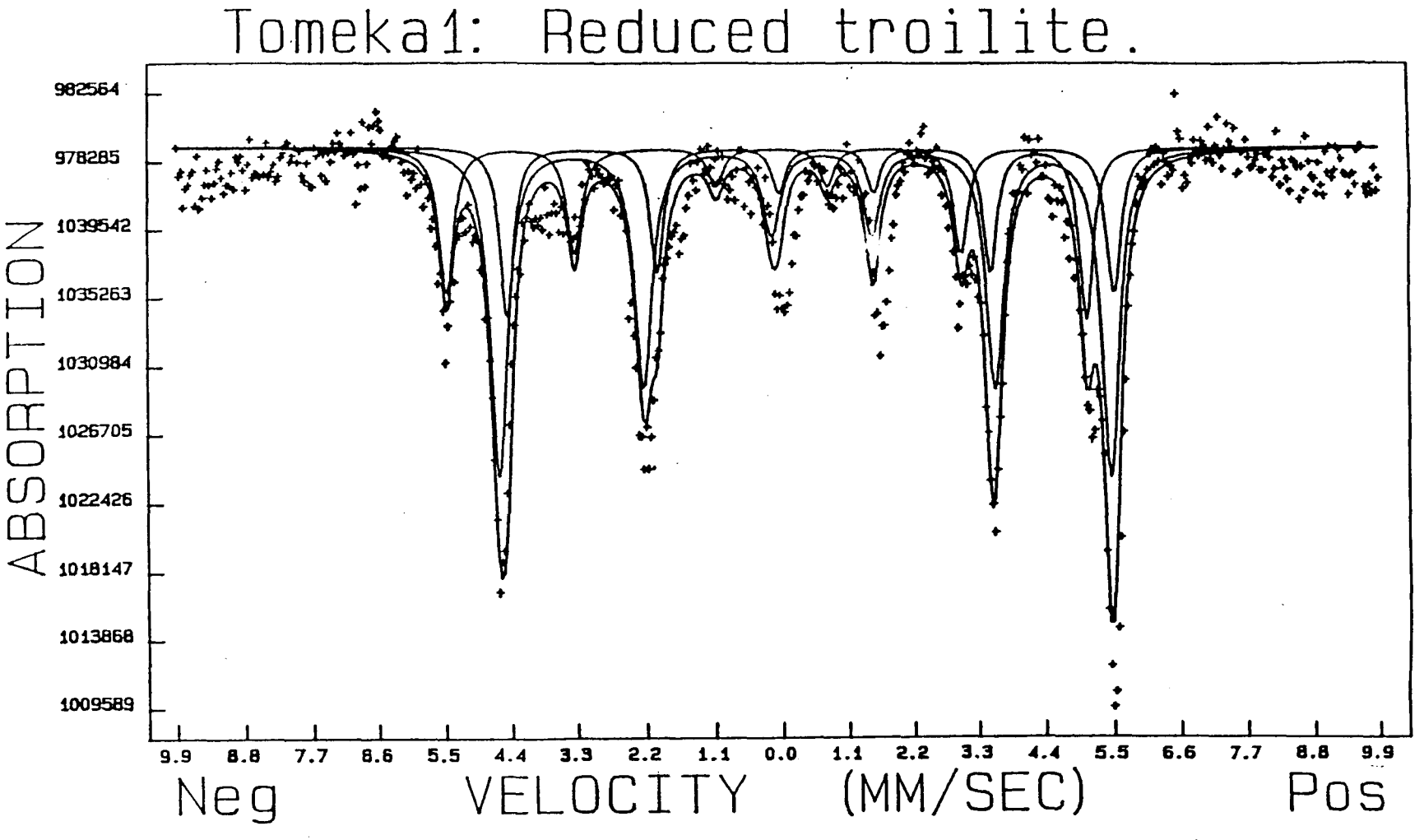

CHI = 1522.08 MISFIT = 4.1120 +/- 0.2797

	INTS	WID	ISO	QUAD	MAG	GY	GX	A1	A2
Iron	0.00293	0.289	0.032	0.1882	340.900	-0.000032	0.000122	0.1856	-0.2063
Troilite	0.00656	0.338	0.655	-0.2380	312.080	-0.000032	0.000122	0.1856	-0.2063
Pyrrhotite	0.00343	0.259	0.630	-0.4406	295.970	-0.000032	0.000122	0.1856	-0.2063

Appendix: Section 4

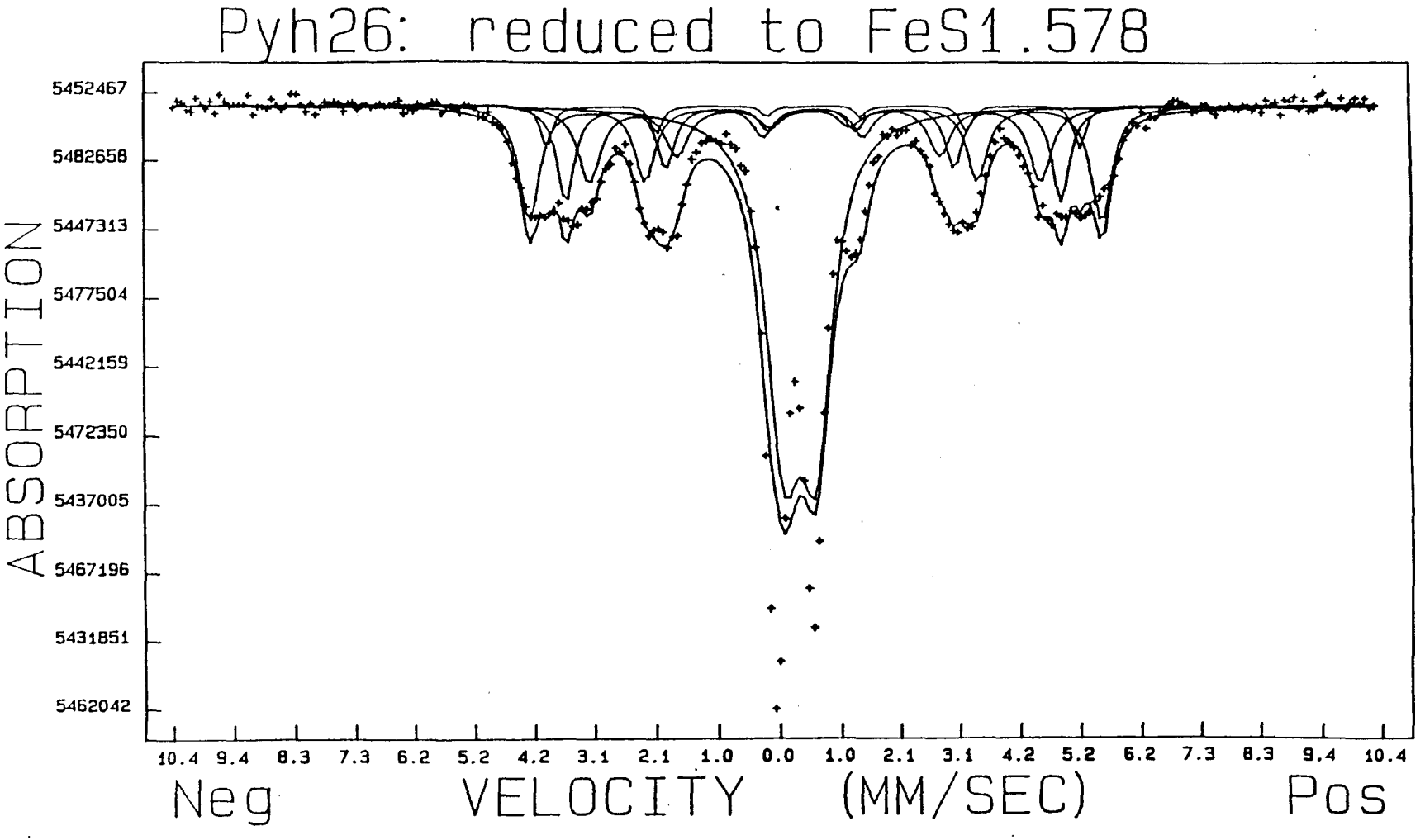

CHI = 770.79 MISFIT = 0.6509 +/- 0.0610

	INTS	WID	ISO	QUAD	MAG	GY	GX	A1	A2
Pyrrhotite	0.00346	0.416	0.729	0.0704	304.520	0.000016	0.000249	-0.0510	-0.2080
Pyrrhotite	0.00129	0.239	0.721	0.0317	283.870	0.000016	0.000249	-0.0510	-0.2080
Pyrrhotite	0.00286	0.359	0.706	0.0687	263.440	0.000016	0.000249	-0.0510	-0.2080
Pyrrhotite	0.00228	0.467	0.702	0.1250	239.670	0.000016	0.000249	-0.0510	-0.2080
Pyrite	0.02715	0.678	0.438	0.5419	0.000	0.000000	0.000000	0.0000	0.0000

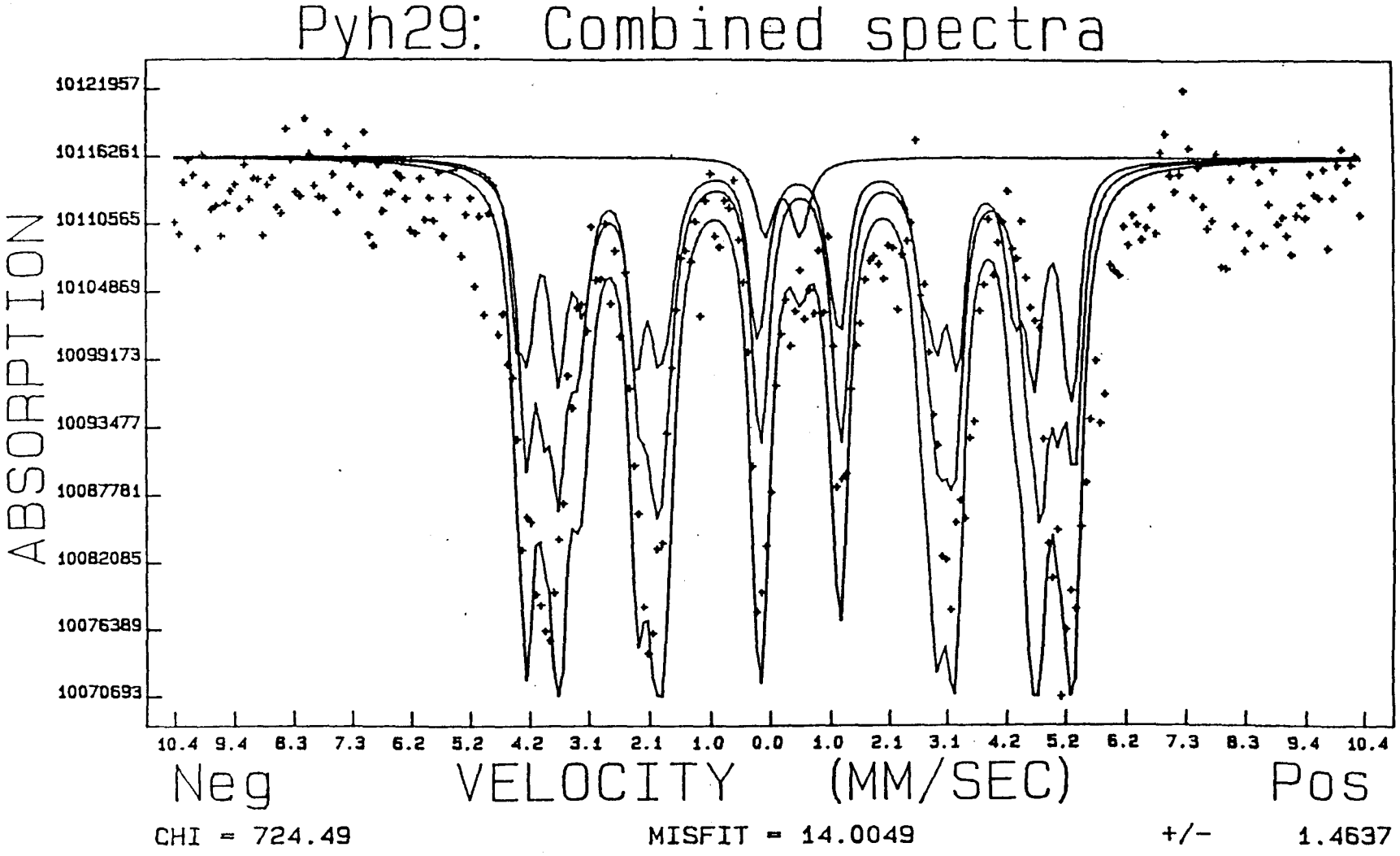

This spectrum was reduced past Fe7S8 and before Fe8S9. The percentage of Fe7S8, which is contained in this spectra, is 40%. There is still some pyrite remaining in the spectra.

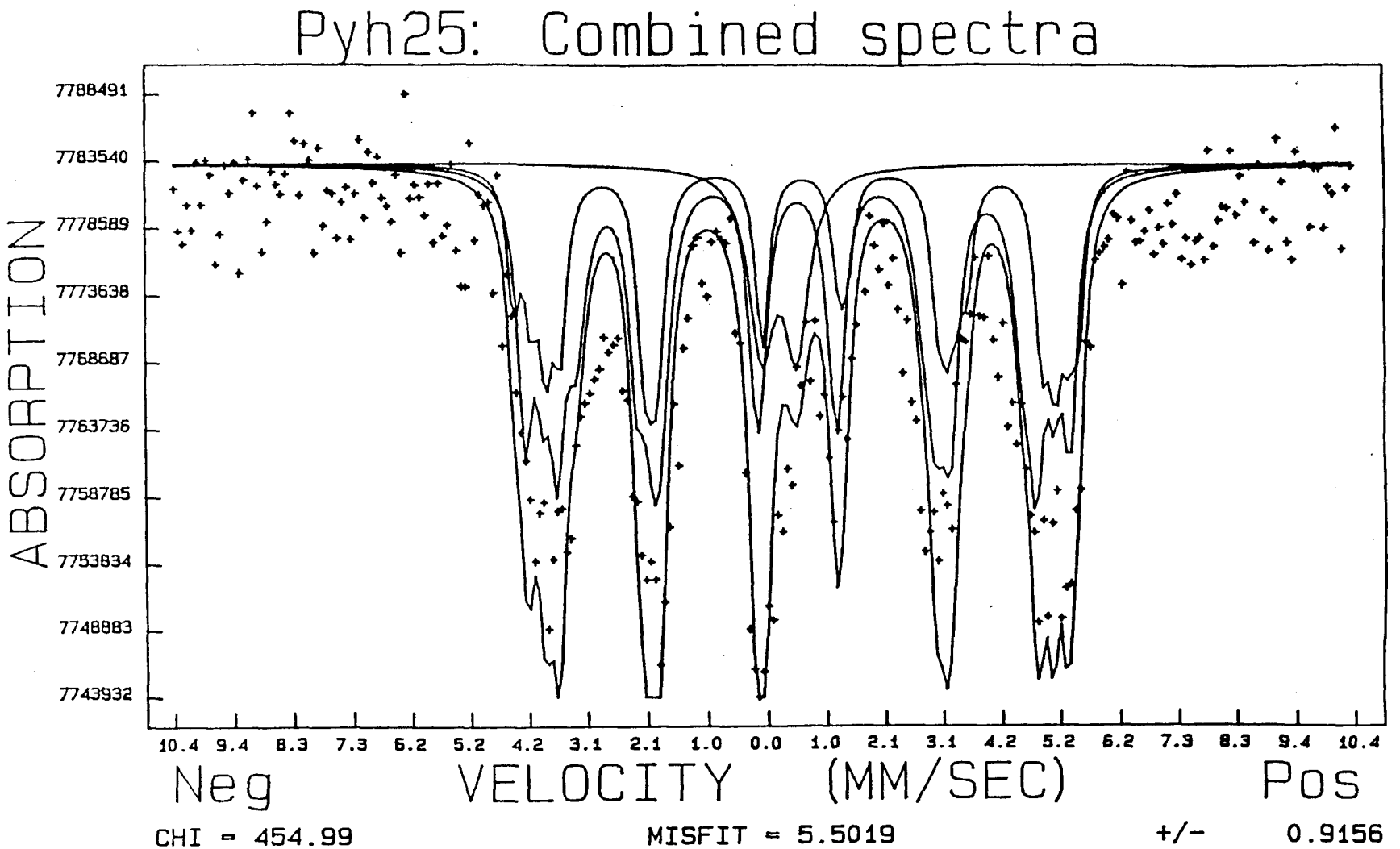

This spectrum was reduced between the inflection points of Fe8S9 and Fe11S12. The spectrum contains 57% of the inflection point Fe8S9. The is also a small amount of pyrite in the sample.

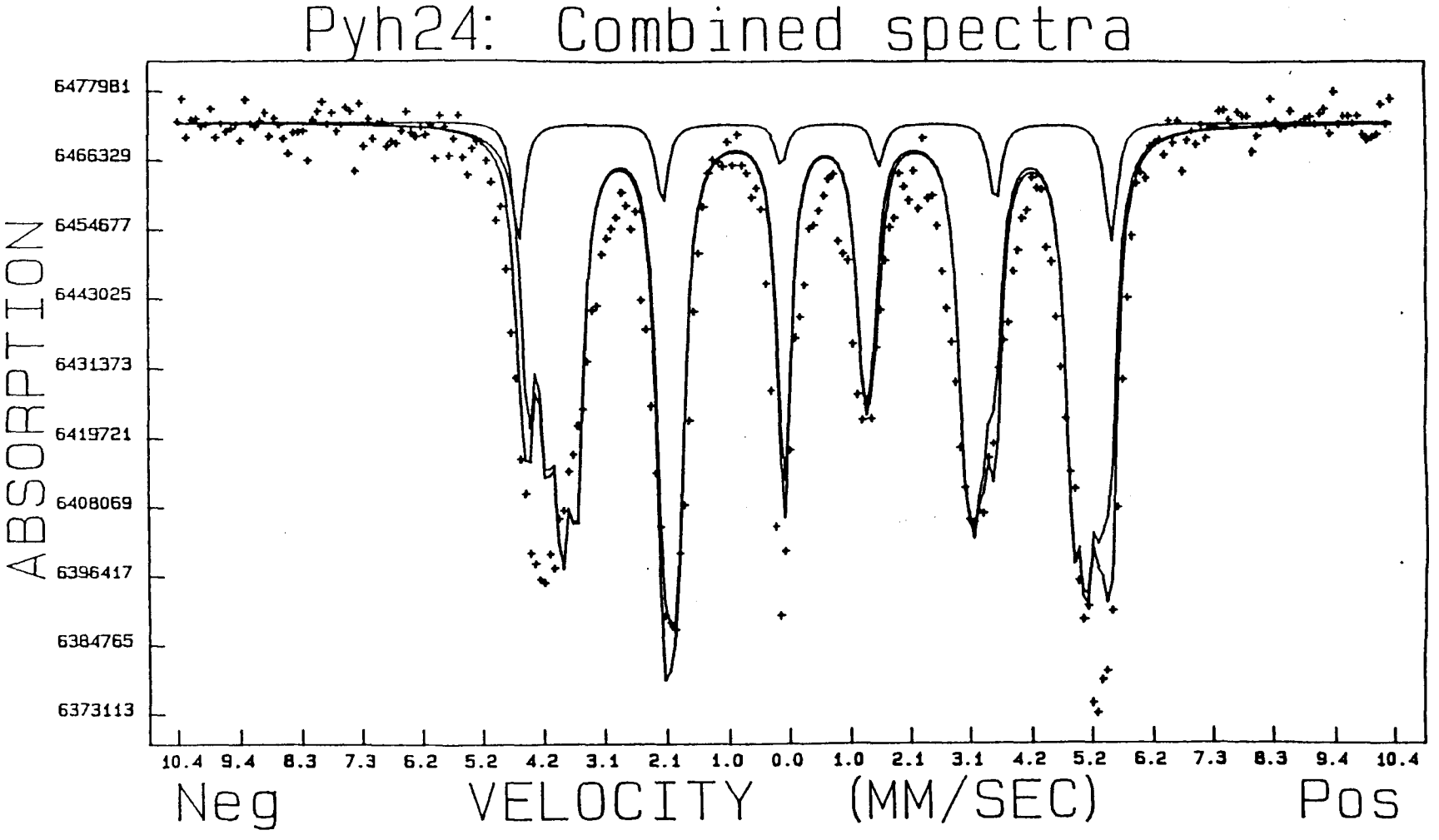

Combined spectra of the last inflection point and troilite. The spectra contains 81% of Fe11S12, which is the last inflection point.

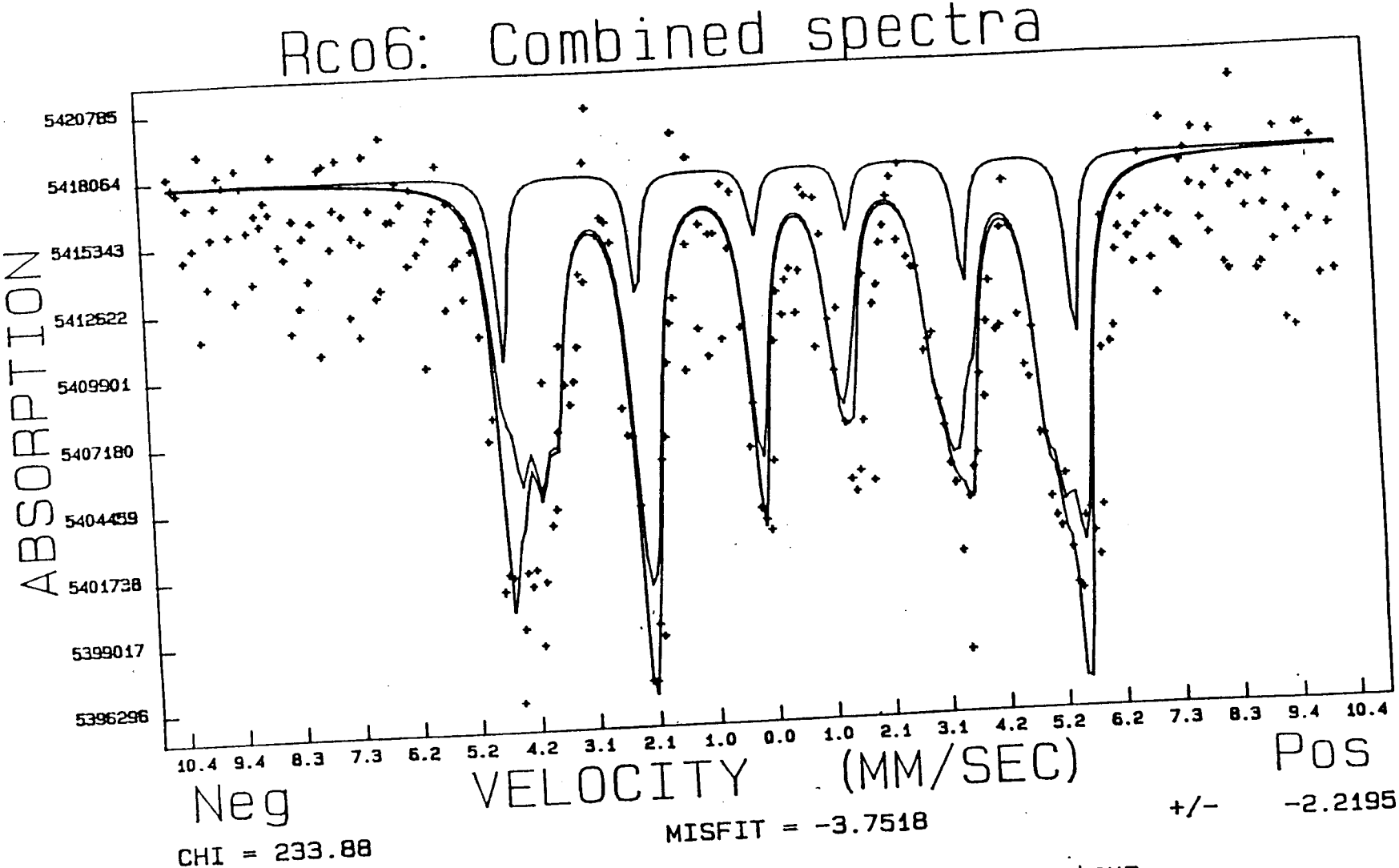

This is a combination of the Fe11S12 and FeS. The spectrum contains 69% of Fe11S12. There is no pyrite remaining in the spectrum.

Appendix: Section 5

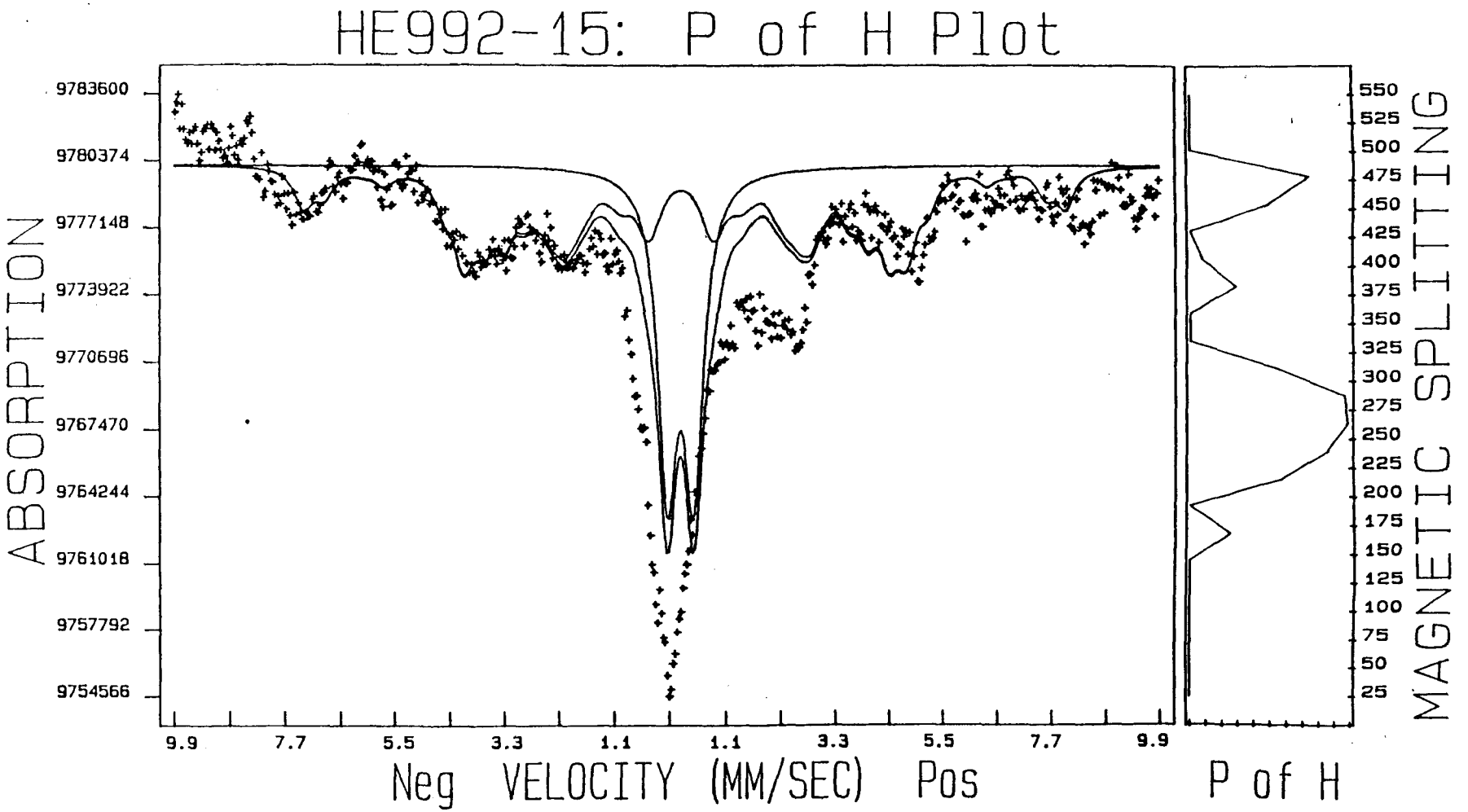

CHI = 198.00 MISFIT = -20.4258 +/- 0.00000

This plot represents the particle distribution at helium temperatures. Isomer shift of 0.64 and quadrupole coupling of 0.05 are used with magnetic splitting increments of 25 from 25 to 550.

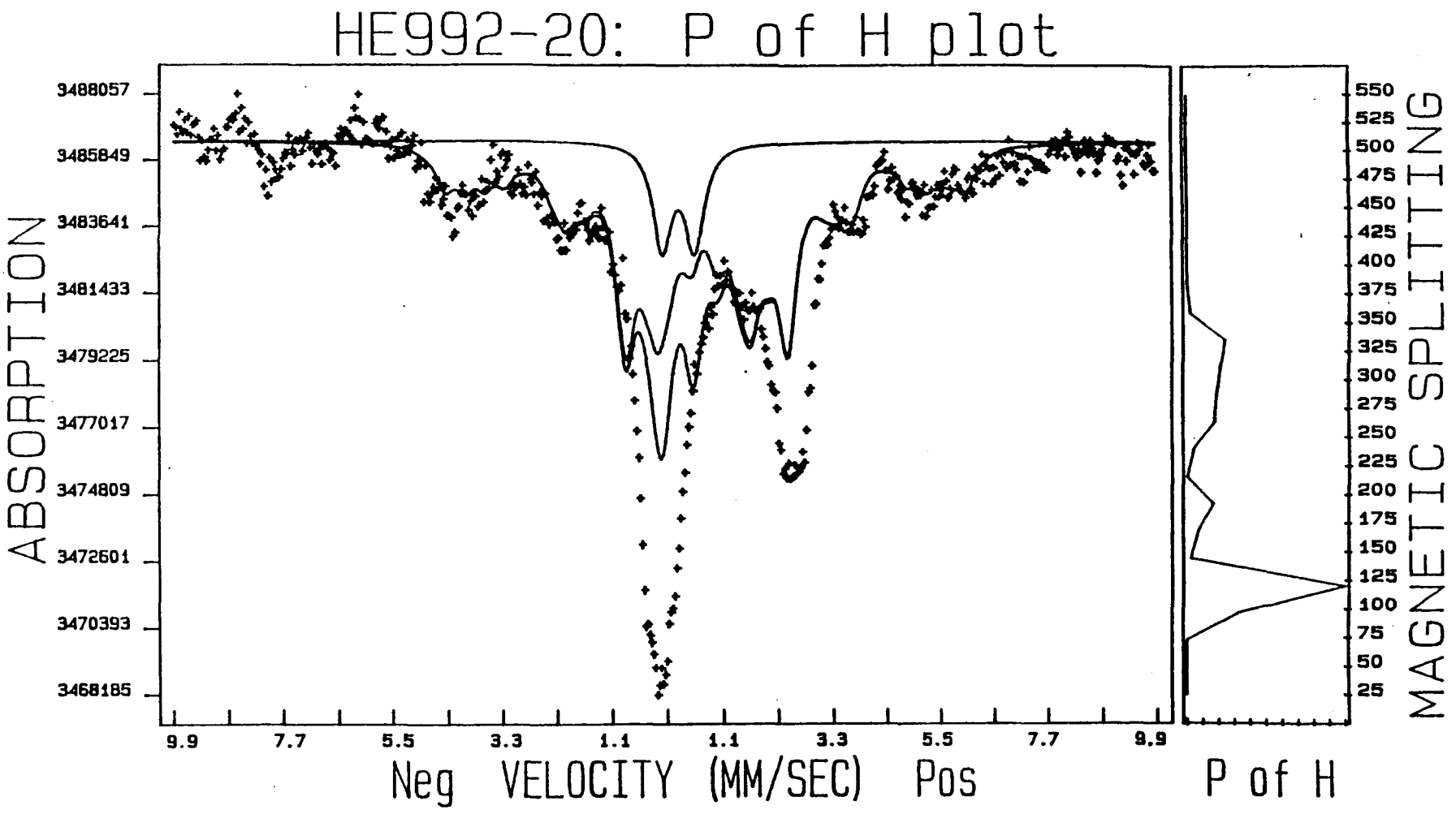

CHI = 528.00 MISFIT = 0.5862 +/- 0.87957

This is a P of H plot for the spectrum HE992-20. The isomer shift value associated to the six-line multiplets is 0.8581, and the quadrupole coupling constant for all the six-line multiplets is 0.0506. The values associated with pyrite are for the isomer shift 0.298 and for the quadrupole 0.5708.

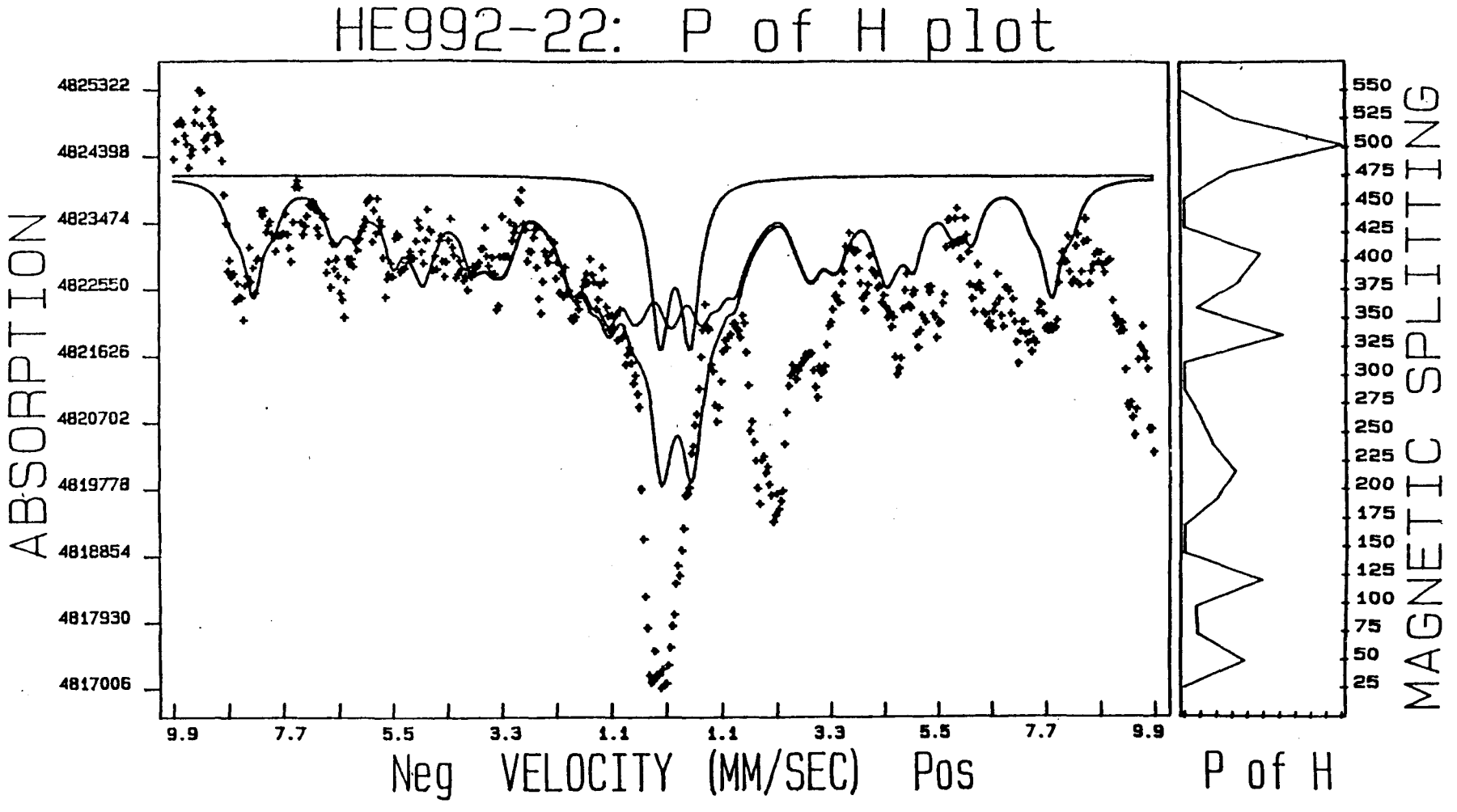

CHI = 81.00 MISFIT = -1063.4440 +/- -675.83241

The isomer shift value related to the six-line multiplets is -0.344. The quadrupole coupling constant is -0.0266. The pyrite has an isomer shift value of 0.295 and a quadrupole coupling constant of 0.598. The P of H indicates the range of magnetic splitting values that are contained in the sample.

Appendix: Section 6

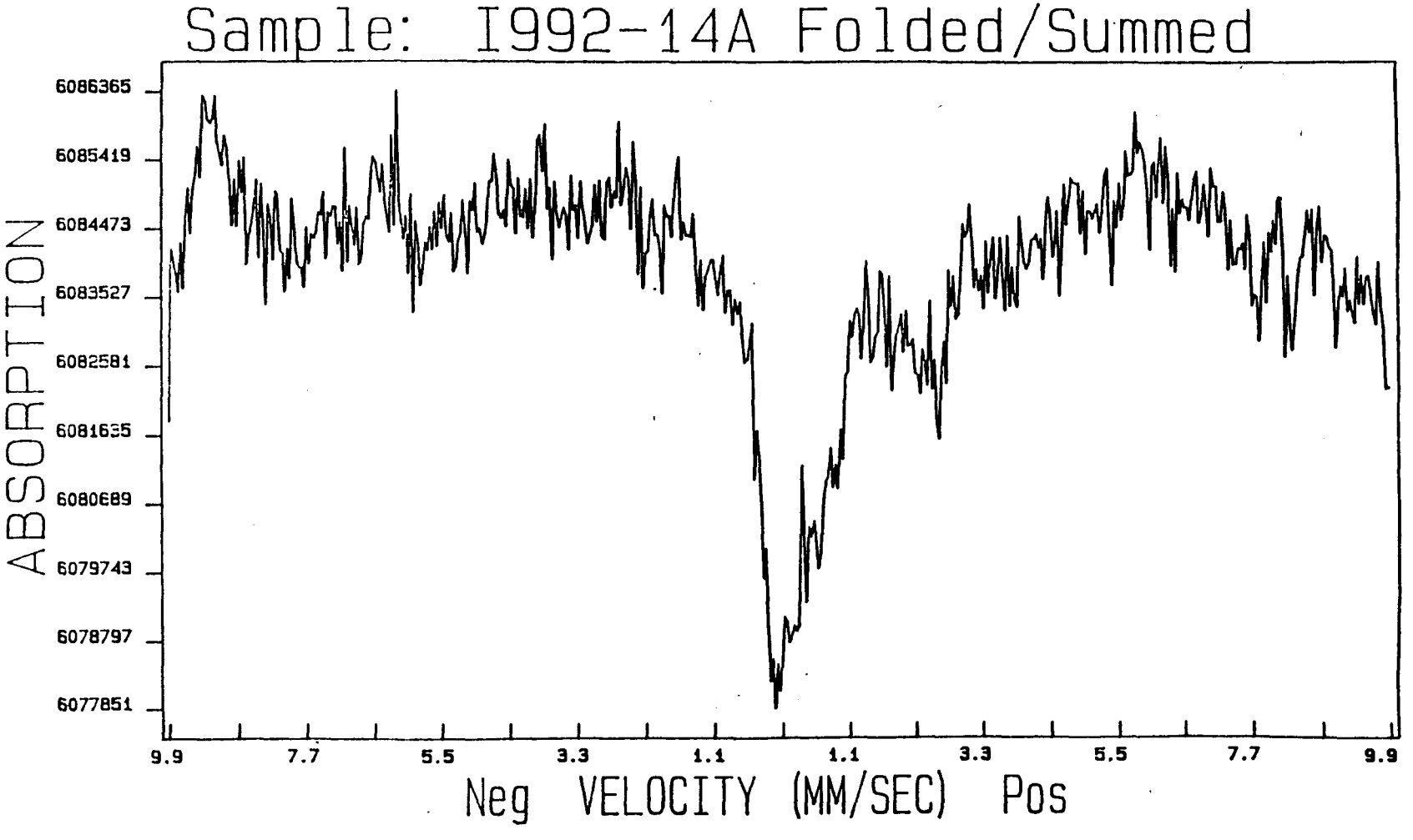

This data is derived from sample I992-14A. It has been folded and summed, smoothed with a digital filter 4 channels wide, and had a sine wave of 22% full scale magnitude passed over to reduce baseline bowing.

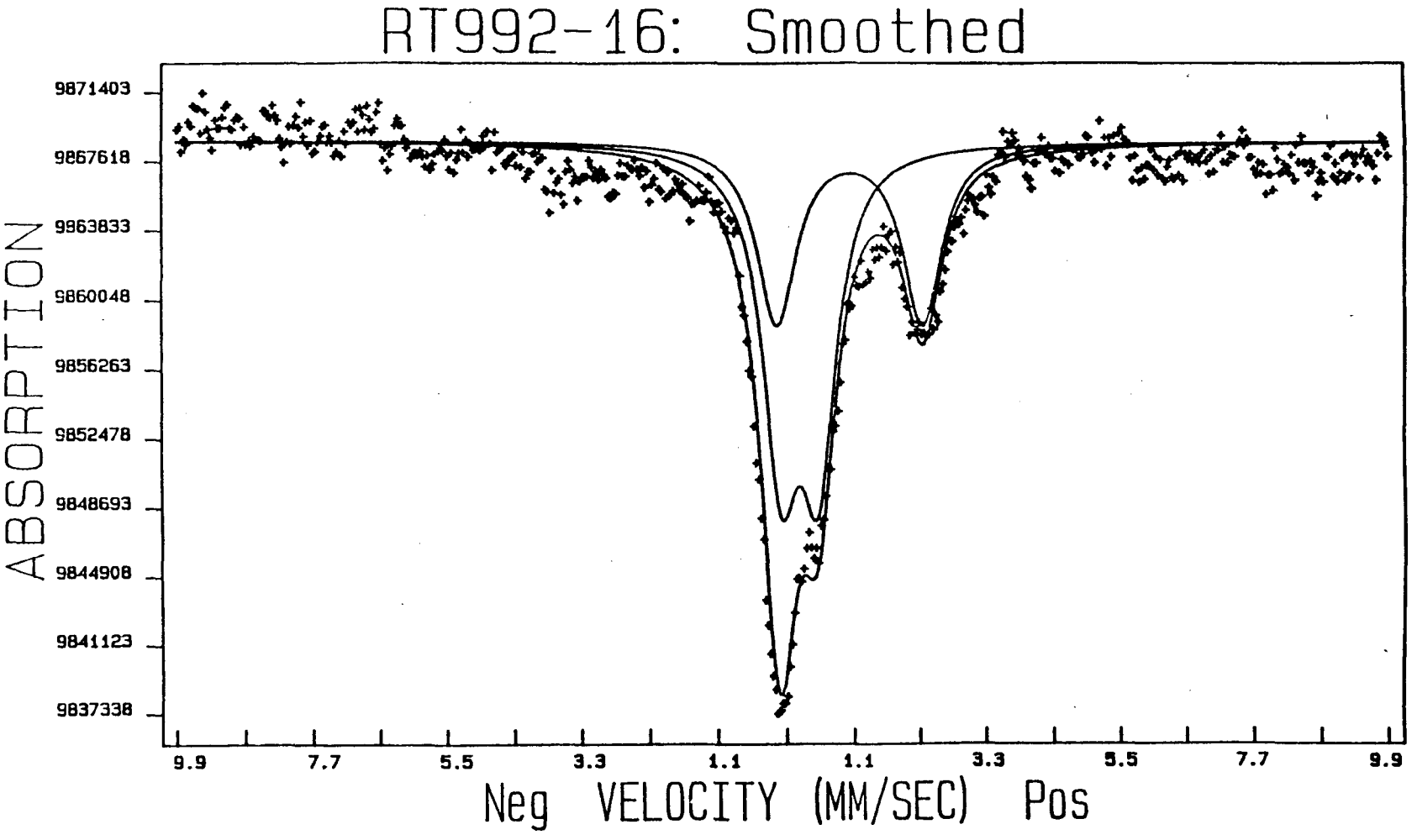

CHI = 2.00 MISFIT = -23.98686 +/- 0.0000%

	INTS	WID	ISO	QUAD	MAG	GY	GX	A1	A2
Pyrite	0.00167	0.699	0.304	0.6020	0.000	0.000000	0.000000	0.0000	0.0000
Ferrous	0.00100	0.780	1.133	2.3934	0.000	0.000000	0.000000	0.0000	0.0000

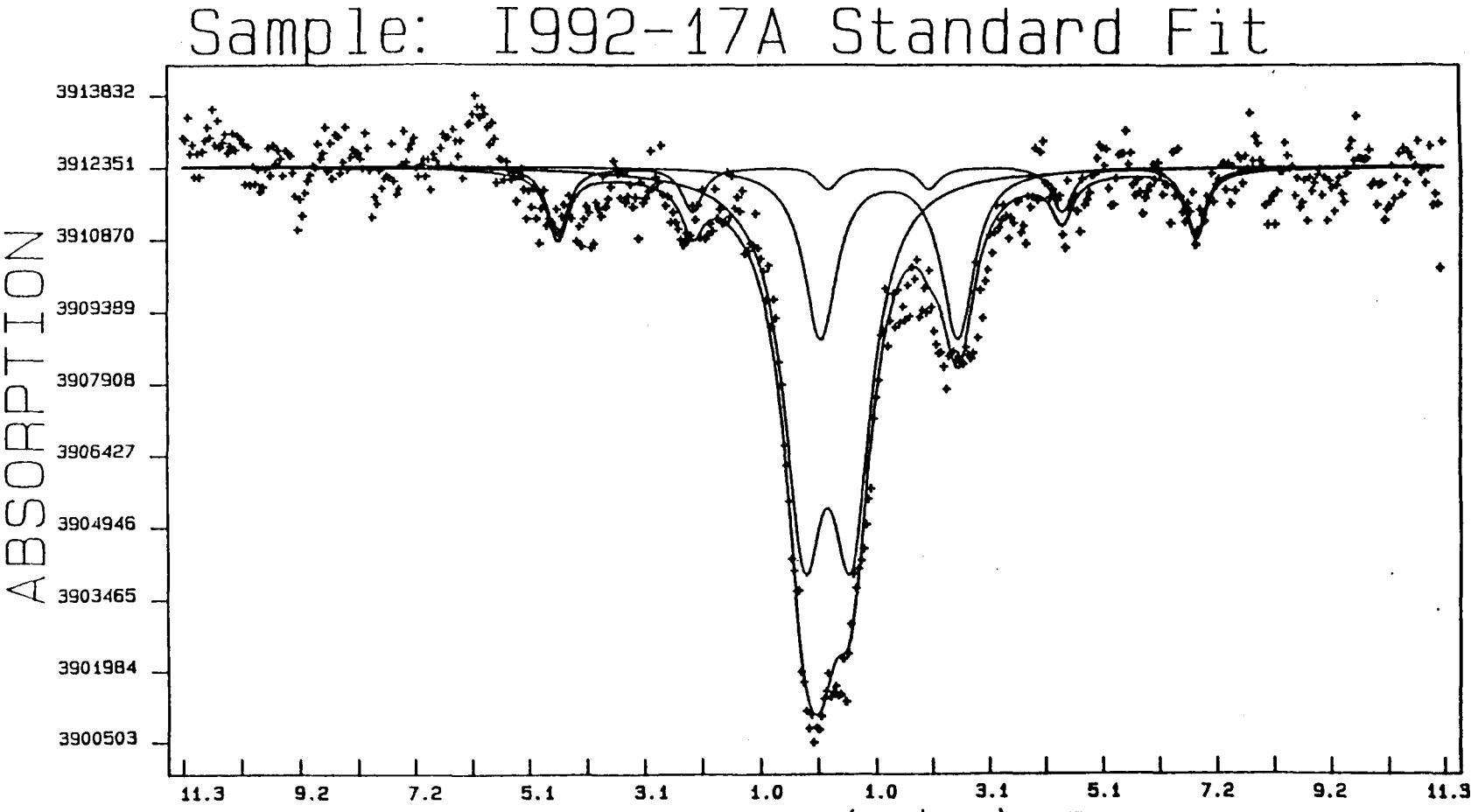

CHI = 1.00 MISFIT = -87.70245 +/- -4.3907%

	INTS	WID	ISO	QUAD	MAG	GY	GX	A1	A2
Pyrite	0.00178	0.850	0.266	0.8400	0.000	0.000000	0.000000	0.0000	0.0000
Ferrous	0.00090	0.700	1.386	2.4600	0.000	0.000000	0.000000	0.0000	0.0000
Oxide	0.00012	0.450	1.206	0.0040	355.000	0.000000	0.000000	0.0000	0.0000

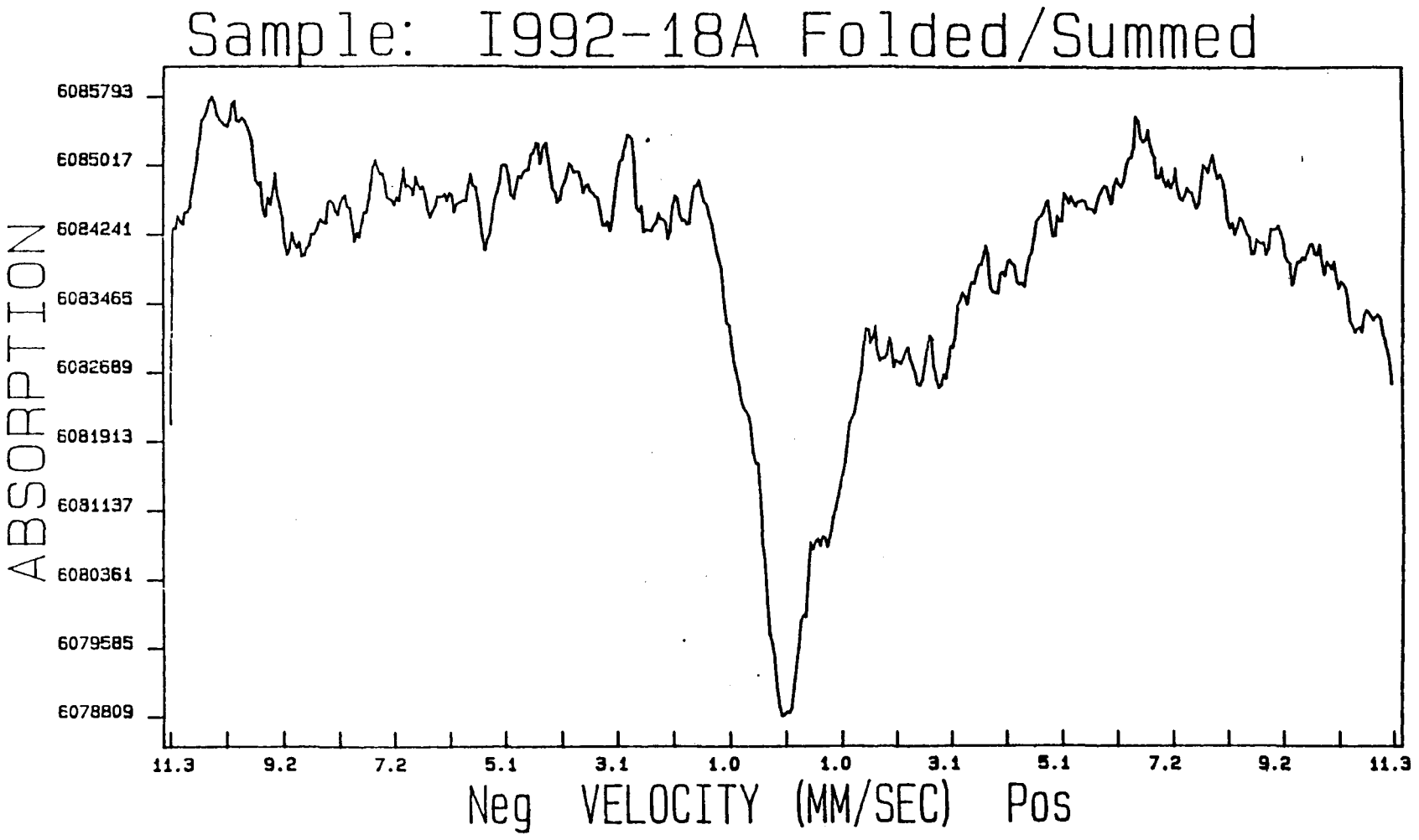

This data is derived from sample I992-18A. It has been folded and summed, smoothed with a digital filter having a width of 4 channels. Further, a sine wave with magnitude of 22% full range has been passed over the data to reduce baseline bowing.

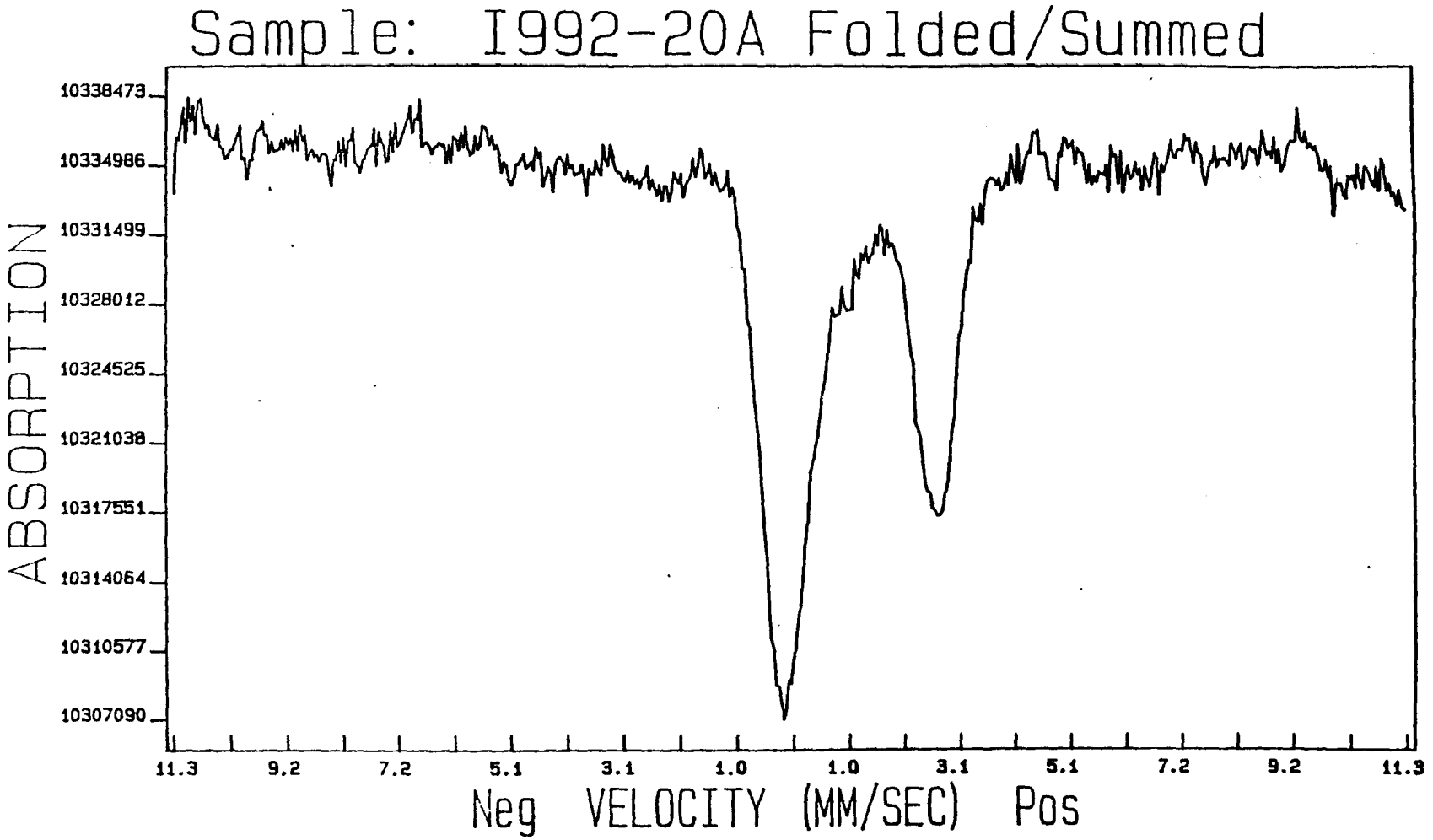

This spectrum is derived from sample I992-20A. It has been folded and summed. A digital filter with a 4 channel width has been passed over the data to remove unwanted high frequencies. Further, a sine wave with 22% full range magnitude has been passed through the data to eliminate baseline bowing.

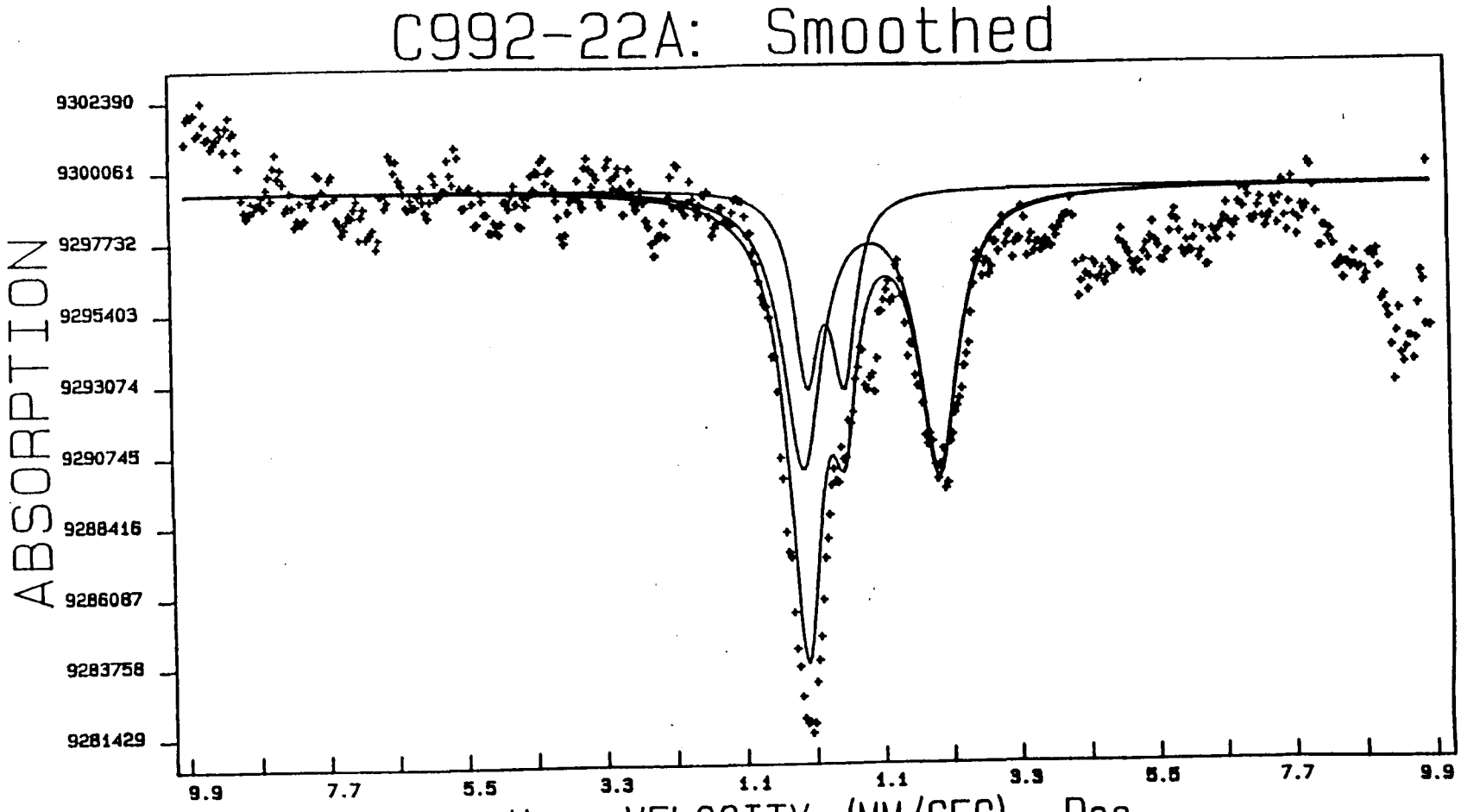

CHI = 50.00 MISFIT = -108.88783 +/- -8.4046%

	INTS	WID	ISO	QUAD	MAG	GY	GX	A1	A2
Pyrite	0.00063	0.468	0.303	0.5934	0.000	0.000000	0.000000	0.0000	0.0000
Ferrous	0.00097	0.735	1.020	2.1722	0.000	0.000000	0.000000	0.0000	0.0000

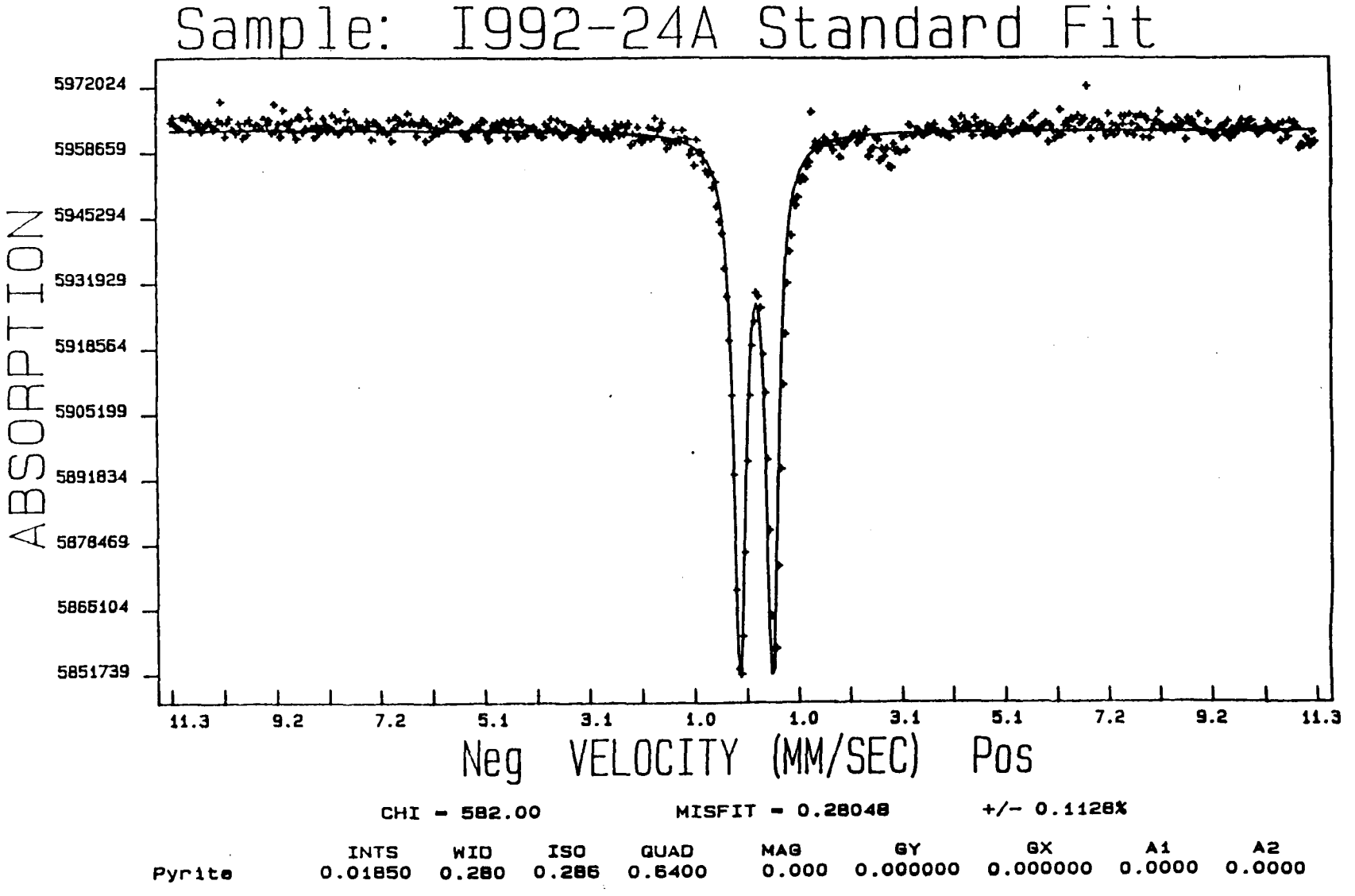
Sample: I992-24A Standard Fit
ABSORPTION
5972024
5958659
5945294
5931929
5918564
5905199
5891834
5878469
5865104
5851739
11.3
9.2
7.2
5.1
3.1
1.0
1.0
3.1
5.1
7.2
9.2
11.3
Neg VELOCITY (MM/SEC) Pos
CHI = 582.00
MISFIT = 0.28048
+/- 0.1128%
INTS WID ISO QUAD MAG GY GX A1 A2
Pyrite 0.01850 0.280 0.286 0.6400 0.000 0.000000 0.000000 0.0000 0.0000

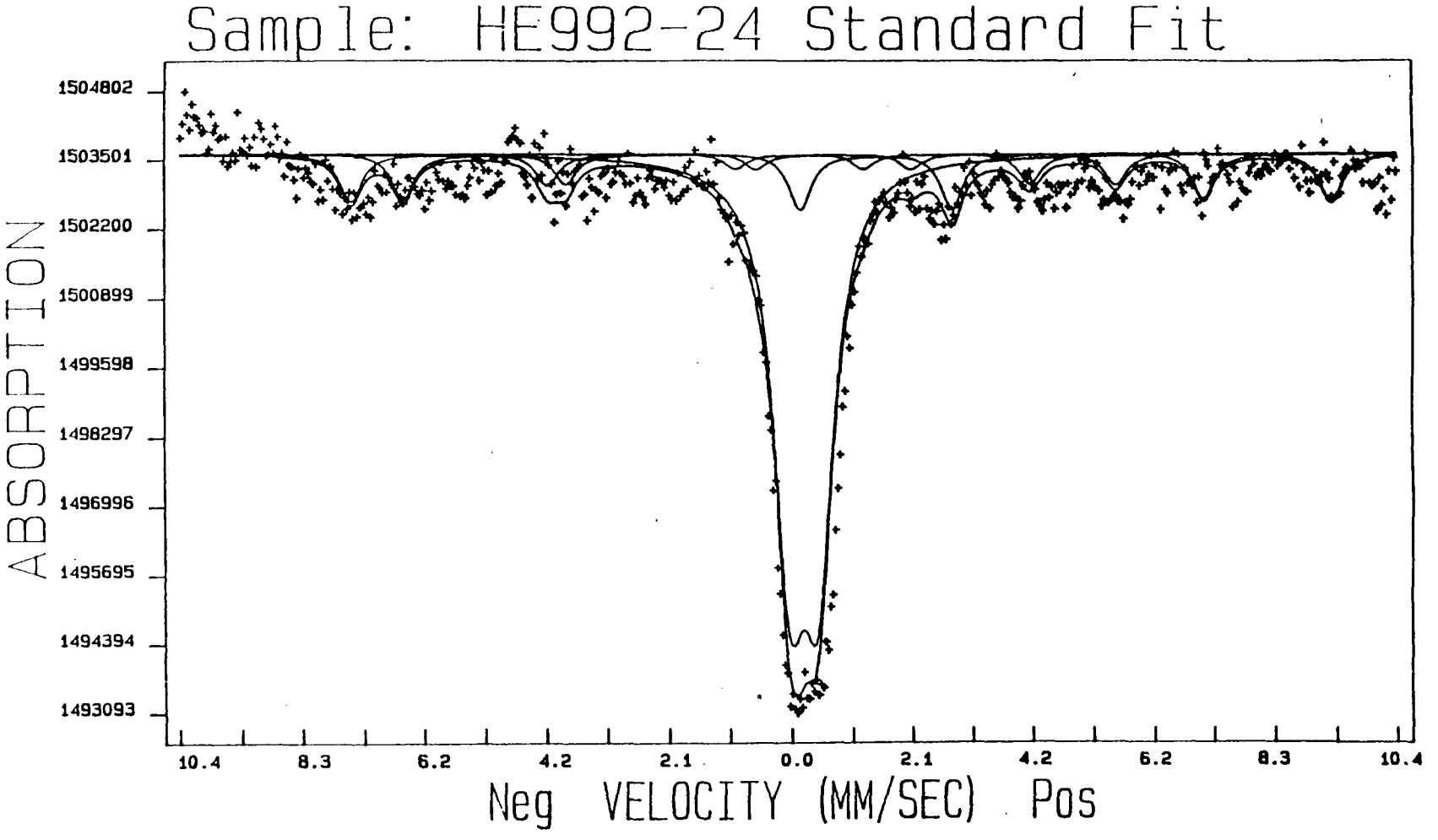

CHI = 15.00 MISFIT = -35.01228 +/- 0.0000%

	INTS	WID	ISO	QUAD	MAG	GY	GX	A1	A2
Pyrite	0.00460	0.650	0.306	0.4800	0.000	0.000000	0.000000	0.0000	0.0000
Oxide	0.00020	0.450	0.906	0.1600	520.000	0.000000	0.000000	0.0000	0.0000
Oxide (2)	0.00019	0.450	0.306	0.1200	425.000	0.000000	0.000000	0.0000	0.0000
Ferrous	0.00070	0.450	1.556	2.6000	0.000	0.000000	0.000000	0.0000	0.0000

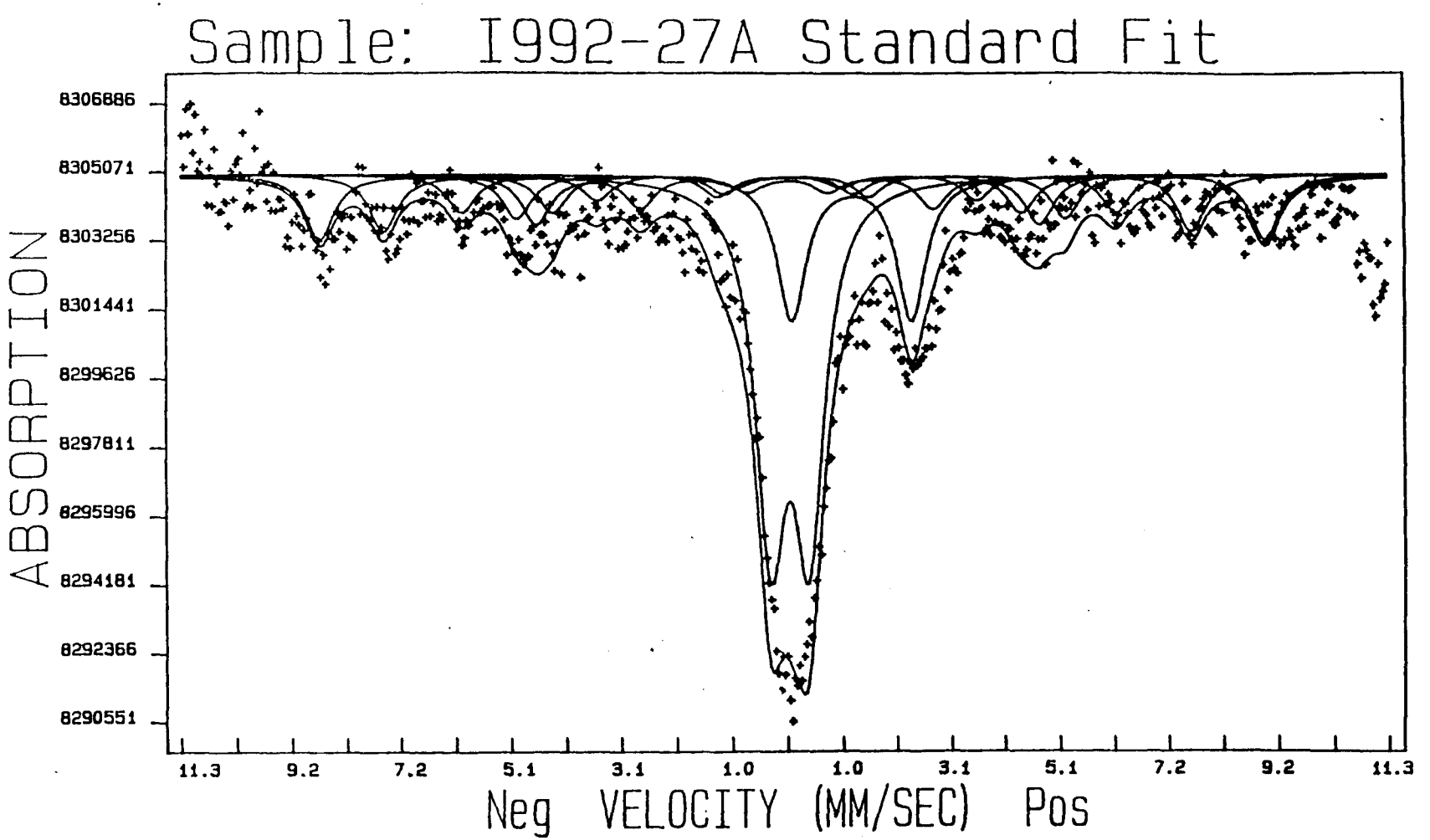

CHI = 4.00 MISFIT = -235.70778 +/- -36.2809%

	INTS	WID	ISO	QUAD	MAG	GY	GX	A1	A2
Pyrite	0.00110	0.680	0.146	0.7200	0.000	0.000000	0.000000	0.0000	0.0000
Ferrous	0.00046	0.650	1.308	2.2400	0.000	0.000000	0.000000	0.0000	0.0000
Pyrrhotite	0.00005	0.650	0.126	0.0400	292.000	0.000000	0.000000	0.0000	0.0000
Oxide (1)	0.00007	0.650	0.226	0.0400	550.000	0.000000	0.000000	0.0000	0.0000
Oxide (2)	0.00006	0.650	0.146	0.0400	470.000	0.000000	0.000000	0.0000	0.0000
Oxide (3)	0.00004	0.650	0.146	0.0400	380.000	0.000000	0.000000	0.0000	0.0000

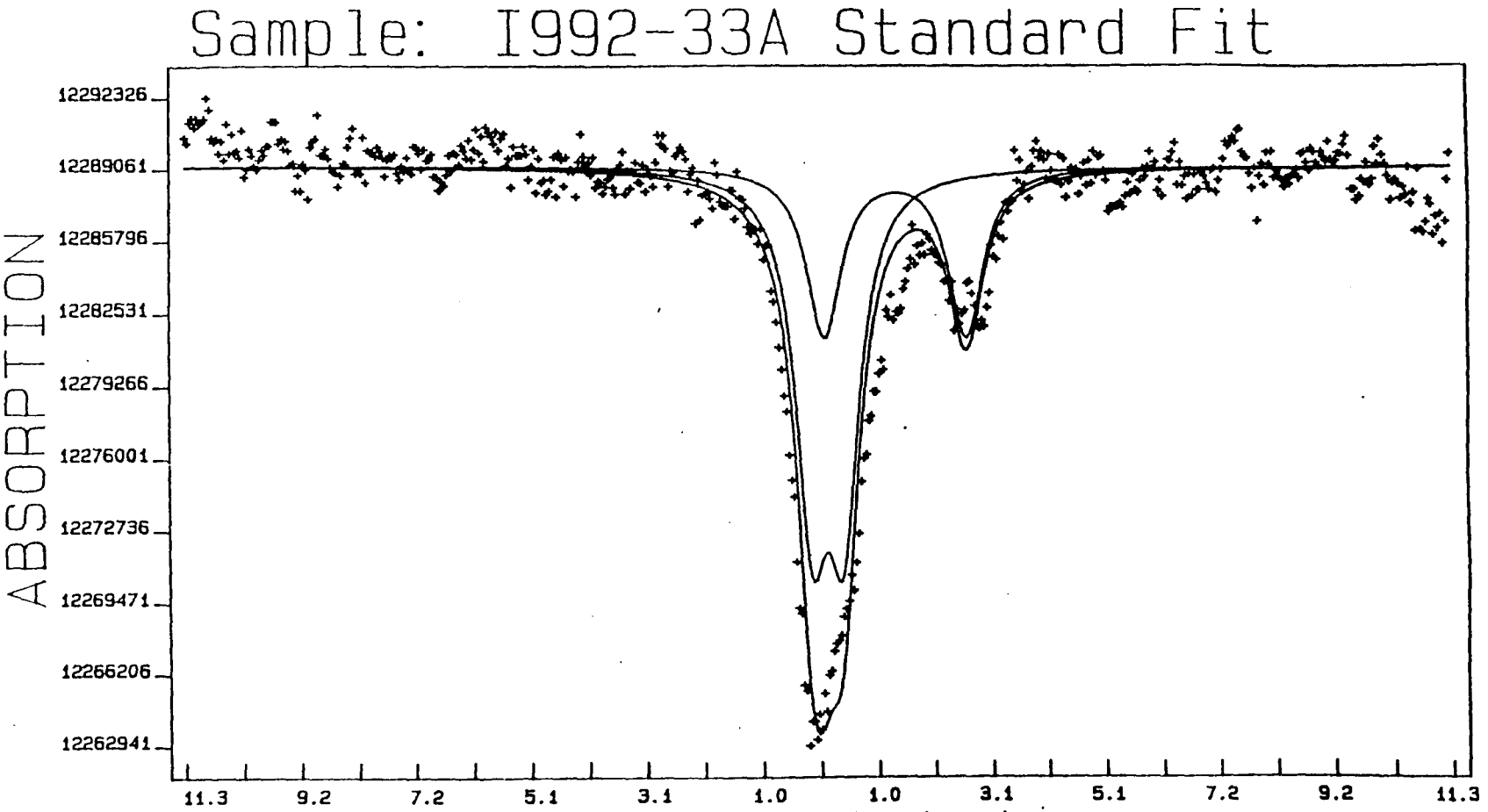

CHI = 8.00 MISFIT = -57.38732 +/- 0.0000%

	INTS	WID	ISO	QUAD	MAG	GY	GX	A1	A2
Pyrite	0.00119	0.680	0.216	0.5600	0.000	0.000000	0.000000	0.0000	0.0000
Ferrous	0.00062	0.740	1.426	2.5400	0.000	0.000000	0.000000	0.0000	0.0000